



Norwegian University of
Science and Technology

Connecting Rod Analysis

Are Nøst

Mechanical Engineering

Submission date: June 2017

Supervisor: Terje Rølvåg, MTP

Norwegian University of Science and Technology
Department of Mechanical and Industrial Engineering

Preface

This paper concludes a master thesis which has been submitted as a part of a MSc degree at the Norwegian University of Science and Technology (NTNU). The work has been carried out at the Department of Mechanical and Industrial Engineering (MTP) during the spring semester of 2017, under the supervision of Professor Terje Rølvåg at NTNU.

The idea to the subject was developed as a natural extension of a project thesis submitted in the previous semester: "Engineer to Order of Connecting Rods." In which it was developed an user template for redesigning existing connecting rod designs, in a module in NX called Product Template Studios.

It is assumed that the reader has a technical background, with knowledge of Finite Element Analysis (FEA) as well as a basic understanding of mechanical engineering. However, the topics covered in this paper will be explained as well as seemed fit, thus a reader without this background can benefit from its content.

I would like to thank professor Terje Rølvåg at NTNU for his guidance throughout this semester, as well as giving me the opportunity to write my master thesis on this subject. I also want to thank Matteo Celeste Bella, CEO of MXRR, for helpful inputs.

Trondheim, 2017-06-11

Are Nøst

Abstract

A virtual testing tool has been created in the FEDEM software by the supervisor, together with MXRR, which enables integrity analysis of the combustion engine, including the connecting rod. However, this test bench does not include contact analysis of the connecting rod. Such an analysis is therefore desired in order to establish the big and small end ovality, thus take strategic steps towards increasing the integrity and performance of the part.

This master thesis describes the approach and results of performing such a contact analysis of the connecting rod. It explores the different simulation methods for this problem, and aims at quantifying the occurrence of ovality, as well as comparing the simulation methods. One linear and one nonlinear solver have been used to perform the analyzes. Necessary and desirable simplifications has been made to improve the analysis efficiency, such as a simplified bearing model. The contact parameters has been carefully investigated to ensure a comprehensive and accurate analysis.

Further, a FEA template has been created in the *Product Template Studios* module in NX. This template aims to streamline the production process of the connecting rod, by making an intuitive GUI for easy simulation set-up. After the template analysis is performed, valuable feedback is given to the user, such as contact pressure and deformation plots.

Sammendrag

Et virtuelt testverktøy har blitt utviklet i FEDEM av veileder, i samarbeid med MXRR. Dette muliggjør avanserte integritetsanalyse av forbrenningsmotoren, inklusiv veivstangen. Denne testbenken inkluderer i midlertidig ikke kontaktanalyse av veivstangen. En slik analyse er derfor ønskelig for å kunne kvantifisere ovaliteten i den store og lille enden av delen. Slik kan man ta strategiske steg for å øke integriteten og ytelsen til veivstangen.

Denne masteroppgaven beskriver tilnærmingen for å utføre en slik kontaktanalyse av veivstangen, samt resultatene. Den utforsker de ulike simuleringsmetodene for å løse dette problemet, og tar sikte på å kvantifisere forekomsten av ovalitet, samt å sammenligne simuleringsmetodene. Én lineær og én ikke-lineær løsningsmetode er blitt brukt til å utføre analysene. Nødvendige og ønskelige forenklinger er gjort for å forbedre effektiviteten av analysene, som for eksempel er et forenklet lager benyttet. Kontaktparameterne er nøye undersøkt for å sikre en omfattende og nøyaktig analyse.

Videre er en FEA-mal opprettet i modulen *Product Template Studios* i NX. Denne malen tar sikte på å strømlinjeforme produksjonsprosessen til veivstangen, ved å lage et intuitivt brukergrensesnitt for å enkelt sett opp en kontaktanalyse. Etter en slik analyse er gjennomført, gis det tilbakemelding til brukeren i form av kontaktrykk- og deformasjonsanimasjoner.

List of Tables

2.1	Characteristics of solid elements	11
4.1	Material composition.	31
5.1	Convergence analysis.	35
6.1	Comparison of KPI's from Load Case 1.	62
6.2	Comparison of KPI's from Load Case 2.	64

List of Figures

2.1	The motion of a connecting rod.	8
2.2	Sections of a connecting rod	9
2.3	Rigid Body Element type 2	12
2.4	The difference between a mesh with and without mesh mating conditions.	14
2.5	Surface-to-Surface Contact variables	17
2.6	Advanced Nonlinear Contact Parameters	18
2.7	The needle roller bearing.	20
2.8	The bush replacement.	21
2.9	The spring-element model.	22
2.10	Modifiaction of bearing material.	24
3.1	Forces acting on the connecting rod.	27
4.1	The five parts of the conrod.	29
5.1	Distortion of mesh (a) and face contact irregularity (b).	33
5.2	Convergence analysis.	34
5.3	The FE model	36
5.4	The RBE2 element replacing the crank shaft.	37
5.5	Cylindrical coordinate system.	38
5.6	The two assigned nodal coordinate systems.	38
6.1	Constraints and load applied to the model (Load Case 2, displayed without the RBE2 element for convenience).	40

6.2	Surface-to-Surface Contact condition.	41
6.3	Contact parameter - 0.03 mm offset.	42
6.4	Load vs time curve for Load Case 1.	43
6.5	The time stepping of the solution.	44
6.6	Strategy parameters.	45
6.7	Nonlinear contact parameters.	46
6.8	Post View modification.	47
6.9	Creation of displacement graph of the big end bore.	48
6.10	Theta values around the big end (similar for the small end).	48
6.11	Displacement graph of the big end ovalisation under compression - SOL 101.	49
6.12	Displacement graph of the small end ovalisation under compression - SOL 101.	49
6.13	Contact pressure (KPI 3 and 4) under compression - SOL 101.	50
6.14	Von Mises stresses (KPI 5 and 6) under compression - SOL 101.	51
6.15	Displacement graph of the small end ovalisation under tension - SOL 101.	52
6.16	Displacement graph of the small end ovalisation under tension - SOL 101.	52
6.17	Contact pressure (KPI 3 and 4) - SOL 101.	53
6.18	Von Mises stresses (KPI 5 and 6) - SOL 101.	53
6.19	Displacement graph of the big end ovalisation under compression - SOL 601.	55
6.20	Displacement graph of the small end ovalisation under compression - SOL 601.	55
6.21	Contact pressure (KPI 3 and 4) - SOL 601.	56
6.22	Von Mises stresses (KPI 5 and 6) - SOL 601.	56
6.23	Displacement graph of the big end ovalisation under tension - SOL 601.	58
6.24	Displacement graph of the small end ovalisation under tension - SOL 601.	58
6.25	Contact pressure (KPI 3 and 4) - SOL 601.	59
6.26	Von Mises stresses (KPI 5 and 6) - SOL 601.	59
6.27	Displacement graph of the big end ovalisation under compression.	61
6.28	Displacement graph of the small end ovalisation under compression.	61

6.29 Comparison between the solvers, showing ovalisation of big end under tension	63
6.30 Comparison between the solvers, showing ovalisation of small end under tension	63
7.1 Designing the template.	66
7.2 The FEA template.	68
7.3 FEA results from the template.	69
7.4 Displacement of big end bore with respect to the cylindrical coordinate system.	70

Contents

Preface	i
Abstract	iii
Sammendrag	v
1 Introduction	1
1.1 Background	1
1.2 Problem description	2
1.3 Objectives	2
1.4 Limitations	3
1.5 Vision	3
1.6 Approach	3
1.7 Structure of the Report	4
2 Theory	7
2.1 The Connecting Rod	7
2.2 Siemens NX	9
2.2.1 Product Template Studios	9
2.2.2 Modelling PTS	10
2.2.3 Simulation PTS	10
2.2.4 Pre-processing tools	10
2.3 Finite Element Analysis	15
2.3.1 SOL 101 Linear Static - Global Constraints	15
2.3.2 SOL 601 Advanced Nonlinear Static	16
2.3.3 Contact Analysis	16

2.4	Simplified bearing model	19
2.4.1	Previous work	20
2.4.2	Comparison and selection of model	22
2.5	Calculation of bearing model characteristics	23
3	Critical load cases and KPI's	25
3.1	Load Cases	25
3.1.1	Load Case 1: Maximum combustion loads	25
3.1.2	Load Case 2: Maximum inertia loads	26
3.2	Key Performance Indicators	26
4	Model description	29
4.1	Contact characteristics	30
4.2	Materials	30
5	Finite Element Model	33
5.1	Mesh Mating	33
5.2	Meshing	34
5.3	RBE2 connection	36
5.4	Nodal Coordinate System	37
6	Finite Element Analysis	39
6.1	SOL 101	39
6.1.1	Boundary Conditions	39
6.2	SOL 601	42
6.2.1	Boundary Conditions	42
6.2.2	Time Step Interval	44
6.2.3	Strategy Parameters	44
6.2.4	Simulation Objects - Surface-to-Surface Contact	45
6.3	FEA results	47
6.3.1	SOL 101	48
6.3.2	SOL 601	54
6.3.3	Comparison	60

7 Product Template Analysis	65
7.1 Post View Templates	65
7.2 Product Template Design	66
7.3 The FEA Template	67
7.3.1 Editing the model	70
8 Challenges	71
9 Conclusion and Suggestions for Further Work	73
9.1 Conclusions	73
9.2 Suggestions for further work	75
A Abbreviations	77
B Risk Assessment	79
Bibliography	81

Chapter 1

Introduction

This chapter describes the background of the chosen topic, and how it has been carried out. The objective of the thesis project will be presented, as well as an approach to complete these objectives. The limitations and obstacles will be briefly discussed in this chapter, followed by the structure of the report. At last, a vision of the desired result will be given.

1.1 Background

The presence of ovality in the big and small end of a connecting rod has a major impact on the integrity of the part, especially in racing applications. A contact analysis is therefore essential for studying the severity of the ovalisation. When conducting integrity analysis of a connecting rod design, Finite Element Analysis (FEA) is the preferred method to incorporate. Siemens NX offers a variety of different solvers which can be used to quantify the desired integrity parameters. For contact analysis, there are mainly two solvers which should be taken into account: SOL 101 and SOL 601, which will be explained later.

An easy-to-use template for conducting FAE can drastically reduce the designing process. NX offers a tool to make such a template called *Product Template Studio*, in which it is possible to create a *Graphic User Interface* (GUI) for a quickly simulation set-up and to get valuable feedback.

1.2 Problem description

The supervisor has together with MXRR and Fedem Tech. AS developed a virtual testing tool for internal combustion engines. This tool is based on the Fedem software that enables accurate integrity analysis of engines including both flexible bodies and control systems.

However, the FEDEM software does not support contact analysis between the big end bearing, the small end bushing, piston pin and the steel insert in a casted titanium rod. The objective with such a contact analysis is to reduce the ovality in both rod ends to increase the integrity of both rods and bearings in racing applications.

1.3 Objectives

In order to perform such an analysis, simplifications to the model have to be considered. The different solvers should be compared and the accuracy measured against the simulation process. Once concluded on a simulation method and desired solver, a FEA template can be created with the desired input and output, focusing on big and small end ovality.

The main objectives in this master thesis are as follows:

1. Study different modelling methods to simplify the model.
2. Identify the involved contact regions in the model.
3. Identify critical load cases in which the connecting rod is subjected to and define KPI's.
4. Explore simulation methods to simulate the load cases in a satisfying way.
5. Develop a FEA template for easy user defined connecting rod simulation.
6. Explore the possibility of using multiple components in the template.

1.4 Limitations

Various challenges and obstacles has surfaced during this thesis work, which has lead to limitations of the work. Nonlinear contact analysis, with interference and play in the SOL 601 solver in NX, demands carefully defining the correct parameters in order to successfully complete a simulation. With limited resources found on similar problems, and acknowledging this was a new field for the author, this analysis has posed some time consuming challenges.

The Product Template Studios module in NX also has some limitations. Although it has been developed with more possibilities though the versions, it still lacks some functions in order to create a complete and detailed analysis template. Using a simulation file created of a assembly model, showed to be difficult, and didn't seem to be supported in the latest version of the PTS.

1.5 Vision

The outcome of the master thesis should in general give a better understanding of simulation methods to capture the occurrence and magnitude of ovality in the big and small end of the connecting rod. It is presumed that the SOL 601 solver will have a greater accuracy than the SOL 101 solver, but with increased CPU time.

The other part of the thesis, the Product Template Analysis, should be a tool for streamlining the production process of the connecting rod. An intuitive GUI is therefore essential for creating a useful template. The possibility to switch from different connecting rod design, thus comparing the analysis between them, would be beneficial.

1.6 Approach

In order to get an overview of the previous explored simulation methods of contact analysis, a study of existing literature on the subject were necessary. Further, selecting the appropriate solvers to explore, regarding the current application and desired results, where done. Acknowledging the importance of a well prepared FE model, as

well as the impact of simplifications of the model, resulted in a highly prioritized FEM understanding. To achieve an accurate simulation, the contact formulation and parameter definition was essential. Understanding the different parameters and their impact of the results, as well as convergence rate, was a crucial part of the work, and a substantial amount time was therefore invested in this.

The analysis part of the Product Template Studios was a new field, with not much resources on the subject online. Some trial-and-error approach must therefore be assumed on this part of the thesis. The knowledge gained during the contact analysis study, was implemented in the PTS, to create a template with the essential features and simulation possibilities, as well as user freedom and customization.

1.7 Structure of the Report

The rest of the rapport is organized as follows:

- Chapter 2 gives an introduction of the nature of a connecting rod as well as the necessary background theory to understand the NX tools and solvers. A simplified bearing model is presented and calculation of modified material properties are performed.
- In Chapter 3 the critical load cases and KPI's is presented.
- Chapter 4 describes the model in question and defines the contact characteristics. An overview of the materials used in the analysis is also presented.
- In Chapter 5, the FE model is described, as well as the essential tools and assumptions to create a well-defined FE model.
- In Chapter 6 the FE analysis is presented. Everything from boundary conditions to time stepping and contact parameters are described. The results of the analyzes is also presented and compared.
- Chapter 7 gives a walk-through of how the Product Template analysis is created and the resulting GUI is presented, with an explanation of its functions and features.

- In Chapter 8 the challenges face in this work is presented and discussed.
- Chapter 9 is the last chapter, where the result of the master thesis is discussed. A conclusion is provided, together with a suggestion of further work.

Chapter 2

Theory

In this chapter, there will first be given a brief explanation of the nature of the connecting rod and its functions. Then an overview of the different NX-tools used in this project work will be presented, as well as a description of the utilization of these tools.

2.1 The Connecting Rod

In an internal combustion engine, there is a beam connecting the piston and the crankshaft. This beam is called a *connecting rod*. It converts the translation movement of the piston, into a rotation movement to the crankshaft, as demonstrated in Figure 2.1 [1].

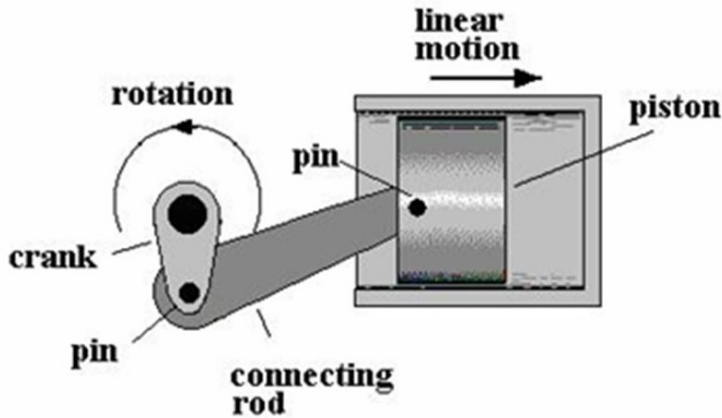


Figure 2.1: The motion of a connecting rod.

There are different cross section designs used to today, but the most common is the I- and H-profile. The connecting rod is considered to be a critical component in racing engines, in terms of mechanical failure, as its often the leading cause of engine failure. The connecting rod is exposed to alternating compression and tension load. Thus, the fatigue properties are an important factor to be considered during the design process.

The OEM connecting rods are usually made from wrought steel or powdered metal. However, in the racing community it has been a growing usage of titanium alloy connecting rods in later years. Increasing the strength and lowering the weight is the key benefits of using titanium [2].

The connecting rod can be divided in three sections: small end, beam and big end, as done in Figure 2.2. The small end is connected to the piston through a piston pin, and the big end is connected to the crankshaft via a bearing. The beam can be, as mentioned, of different profiles, but the H-profile is considered in this figure, as well as in this project in its entirety.

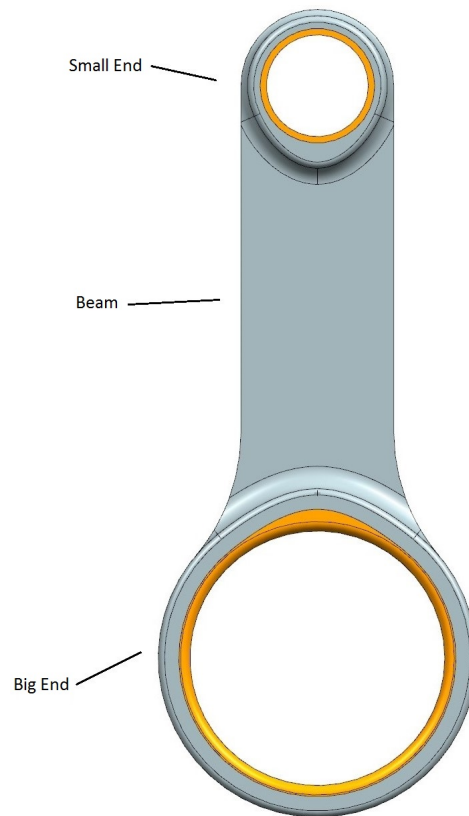


Figure 2.2: Sections of a connecting rod

2.2 Siemens NX

Siemens NX is an advanced PLM (Product Lifecycle Management) software which provides the capability to do product design, integrity analysis, as well as manufacturing solutions.

2.2.1 Product Template Studios

The Product Template Studios (PTS) module is a tool integrated in NX 10 and 11 (it was a separate program in earlier versions), where one can create a Graphic User Interface (GUI) with controllable parameters. The purpose of using PTS is to create templates for easy design modifications or simulation set up, which will increase efficiency in product design and integrity analysis.

The Product Template Studios uses a simple drag-and-drop functionality, making it an easy to use tool with no need of programming experience.

2.2.2 Modelling PTS

Since a design methodology is often individual from person to person, modifying a model can lead to difficulties when another designer tries to work on the model. With a PTS created template, these complications are eliminated. Even an inexperienced NX user can easily make design changes through an intuitive user interface. With a parametrically controlled design, one can with the PTS create a GUI constructed to make predefined design changes.

It is also possible to switch between different design, by the use of *suppression by expression*. The suppression tool in NX gives the user the opportunity suppresses desired features or solids in the model. This is nothing unique, but the *Suppression by Expression* feature enables us to control the suppression by a defined expression. It allows the user to toggle the different designs by connecting the suppression to an “on and off” (0 or 1) expression. Thus, controlling if a feature/solid should appear or not, or vary between two or several features/solids. In this project, it is desired to be able to switch between different connecting rod designs, in order to run various analysis on these.

2.2.3 Simulation PTS

In the Product Template Studios, it is also possible to create a template for the simulation module in NX. This feature is an important part of this master thesis. After creating a simulation file, it can be imported into the PTS, and a GUI can then be developed with the desired parameters, such as load, constraints, element size, etc. In order to get a visual output from the GUI, it is necessary to run a simulation and save the desired *post view* as a template. Either a displacement representation, Von Mises stresses or other.

2.2.4 Pre-processing tools

Preparing the CAD model for simulation is done in the pre/post-processing application in NX. Creating a FEM model, can include the use of different dimensional elements,

e.g 0D, 1D, 2D and 3D, as well as various meshing tools. The tools applied in this thesis will now be presented.

Solid Elements

Three-dimensional element, or "Solid Elements", are used to build a FEM model of a solid structure, where the three-dimensional nature of the model is essential to capture. The connecting rod is indeed such an element. The solid elements are only defined by three degrees of freedom: translations along each axis. Whereas two-dimensional elements on the other hand is defined by six: translations and rotations. A hood of a car is an example of a structures which would benefit from using shell elements, as the geometry of this structure could easily be represented by two-dimensional elements [3].

The main difference between the solid elements is the number of faces and connected nodes, as well as the shape of the element. Table 2.1 categorizes the available solid elements and their differences:

Element Type	Nr of nodes	Nr of faces	Shape
CTETRA	4-10	4	Tetrahedral
CHEXA	8-20	6	Brick
CPENTA	6-15	5	Wedge
CPYRAM	5-13	5	Pyramid

Table 2.1: Characteristics of solid elements

As seen in the table above, the elements has a variable number of nodes. This is because one has the option to include midside nodes or not. Generally, including a higher number of nodes, gives more accurate results, but increases the CPU time.

The most commonly used element type is the **CHEXA** element. It gives the most accurate stress data recovery, and has a superior 20 node capacity. However, if the element is distorted, the accuracy decreases [3]. Therefore, in some cases, other element types might be a better choice. This includes structures which has sharp turns, fillets and other complex geometry. The **CTETRA** element is a preferred option to deal with such complexity in the geometry, which is the case for the connecting rod. It should, however, be specified with 10 nodes configuration when solving structural problems.

The four-noded CTETRA-element is exceedingly stiff, and should be limited to heat-transfer applications. Both the CTETRA and CHEXA elements output stresses based on calculation from the center of the elements and Gauss points.

RBE2 element

A *Rigid Body Element* type 2 (RBE2) is an element that consists of one independent node, a so-called master-node, connected to one or several dependent nodes, or slave-nodes. The degrees of freedom is specified at the master-node, and the slave-nodes are thereby dependent of the specified constraints. By the use of constraint equations, the motion of the master-node are directly coupled to the motion of the slave-nodes. A simplified stiffness-matrix is achieved as the RBE2 elements does not contribute directly to the matrix [3]. The application for a RBE2 element is wherever a simplified rigid connection is desired. Nonetheless, the RBE2 element can create unnatural stiffness in the structure, as the connection is infinite stiff. Therefore, it should be used where the stiffness indeed can be assumed infinite stiff, compared to the rest of the structure, and it does not affect the results in an undesirable way. It should be accounted for the increased stiffness it presents. Figure 2.2 gives a visual description of the RBE2 element.

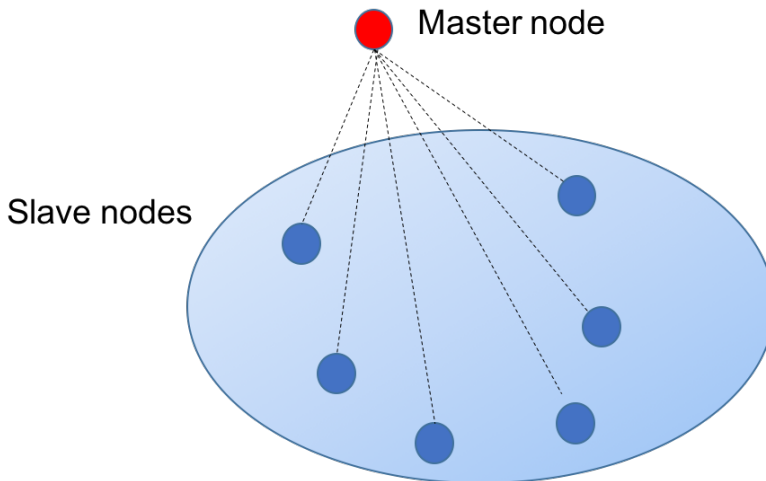


Figure 2.3: Rigid Body Element type 2

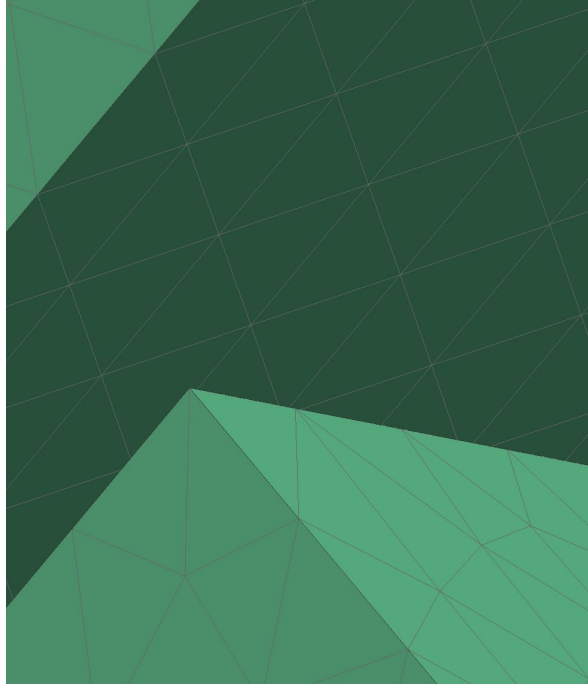
Mesh Mating

Mesh mating is a tool available in the FEM environment that can be used to create coincident meshes between parts, resulting in a continuous FE model. It aligns, merges and/or connects the nodes of the contacting surfaces, thus satisfying the displacement continuity of the involved parts [4]. There are three types of mesh mating:

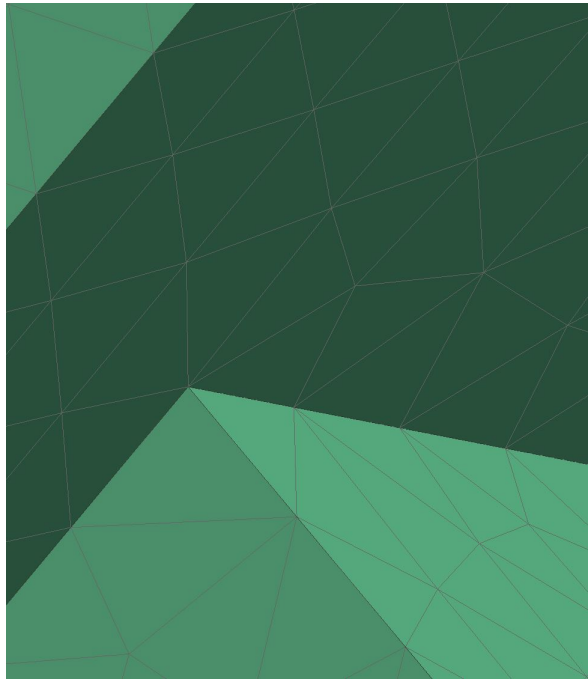
- Glue Coincident Condition
- Glue Non-Coincident Condition
- Free Coincident Condition

With *Glue Coincident Condition* mesh mating assigned to the geometry, the two faces will share the same node when the mesh is created and the faces in contact are identical. *Glue Non-Coincident Condition* creates displacements constraints between the nodes in a discontinuous mesh to connect the surfaces. The *Free Coincident Condition* however, aligns the meshes of the two bodies (or sheets), but does not create any connection between the nodes. It merely creates duplicate nodes with the same locations. This option is used whenever contact interaction is desired, and later specified. Figure 2.4 shows before and after the mesh mating condition *Free Coincident* is used between two bodies.

Mesh mating can either be *automatically* or *manually* assigned. With automatic creation, NX searches the model for contacting surfaces, and assigns the chosen condition to it. With manual creation, however, the user defines which surfaces to mesh mate, which can give better accuracy of the mesh mating.



(a) Before assigning mesh mating condition.



(b) After updating with *Free Coincident Condition*.

Figure 2.4: The difference between a mesh with and without mesh mating conditions.

Nodal Coordinate System

The displacements and locations of the nodes of which the FE model consist of, are by default calculated with respect to the *Global Coordinate System*. However, it could be advantageous in some cases to assign a separate user-defined coordinate system to the model, for which the locations and displacements will be calculated as well [5]. There are two types of nodal coordinate systems that can be assigned to the model:

- Nodal **reference** coordinate system
- Nodal **displacement** coordinate system

The nodal reference system allows the user to get node locations with respect to the defined coordinate system, thus being able to move the nodes by altering the position of the reference coordinate system.

With a nodal displacement system assigned, the nodal-displacements are written with respect to this, and not the global coordinate system. This can be used to specify nodal displacement constraints, as well as displaying the displacement solver output with respect to the defined coordinate system.

In both cases, the defined coordinate system can be either cartesian, spherical or cylindrical.

2.3 Finite Element Analysis

Siemens NX offers a variety of different solution methods to solve most structural analysis problems, both linear and nonlinear analysis. The solvers implemented in this master thesis is the linear static solver *SOL 101 Linear Static – Global Constraints*, as well as the advanced nonlinear solver *SOL 601 Advanced Nonlinear Statics*. They will be explained briefly below.

2.3.1 SOL 101 Linear Static - Global Constraints

As mentioned, SOL 101 is a linear static solution, meaning it assumes linear material behaviour, e.g. no yielding beyond the yield limit. It is also assumed that the evolved deformation is at a level considered small, in comparison to the dimension of the model

in use. However, the solver does account for some nonlinearities, e.g. contact, which has been exploited in this master work [6].

2.3.2 SOL 601 Advanced Nonlinear Static

The SOL 601 solver is suitable when the nonlinearities can't be neglected. In the case where parameters such as structural stiffness, material properties and contact is a function of displacement, the problem becomes nonlinear. In the presence of large deformation, a linear static solution may be insufficient in solving the problem in an accurate and satisfying way. The nonlinear analysis is considering nonlinear behaviour due to geometric and material nonlinearities. In comparison to SOL 101, this analysis requires more computation power, resulting in a longer analysis time.

2.3.3 Contact Analysis

Both SOL 101 and SOL 601 supports the use of contact formulations in their solutions. These contact formulation are defined pre/post module in the simulation file as a *Simulation Object Type* called *Surface-to-Surface Contact*. The figure below shows the Surface-to-Surface Contact window where one defines the relevant contact pairs (Figure 2.5). This can be done either by *Automatic Pairing*, where NX locates the contacting surfaces in the model and automatically defines contact formulation between them, or *Manual*, by selecting the desired surfaces on the model.

Further, *Contact Region Parameters* can be defined, such as source/target offset in order to create an initial gap or interference between the contact surfaces. *Coefficient of Static Friction* is defined in the *Contact Set properties* and is an absolute necessity when a non-constrained body is in contact with a constrained body in order to maintain a stable model. At last, *Local Contact Pair Parameters* can be defined in order to increase both contact accuracy and convergence of the model. When running a linear analysis, such as SOL 101, these parameter has little to no effect on the analysis performed in this project. However, the *Advanced Nonlinear* (BCTPARA) parameters, shown in Figure 2.6, has been greatly tweaked in order to increase accuracy and convergence in the analyze of the connecting rod.

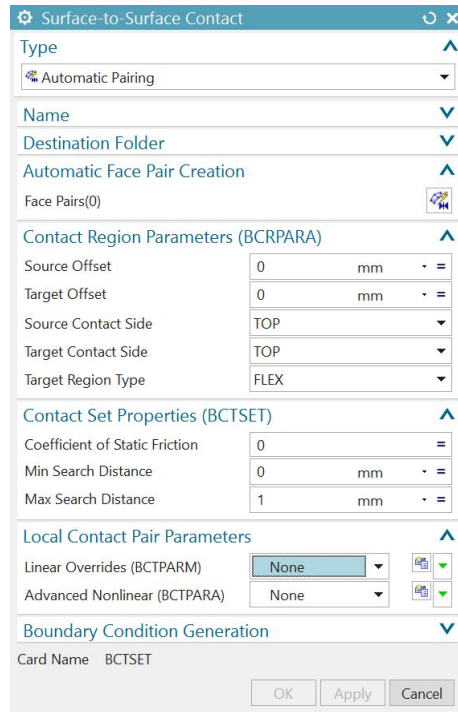


Figure 2.5: Surface-to-Surface Contact variables

Not every parameter has been edited relative to the default value in this thesis, and only the parameters of interest will be explained below:

Constraint Algorithm

The solver used in SOL 601 is ADINA solver, which offers three different algorithms for contact solutions [7]:

- **Constraint-function method** – replaces the ideal contact constraints with non-ideal constraints by implementing a constraint function. This function is differentiable and does not involve any inequalities.
- **Segment (Lagrange multiplier) method** – introduces Lagrange multipliers to enforce the contact conditions and are used with ideal contact constraints.
- **Rigid target method** – this method is a simplified contact algorithm and is specifically intended for stamping problems and metal forming applications.

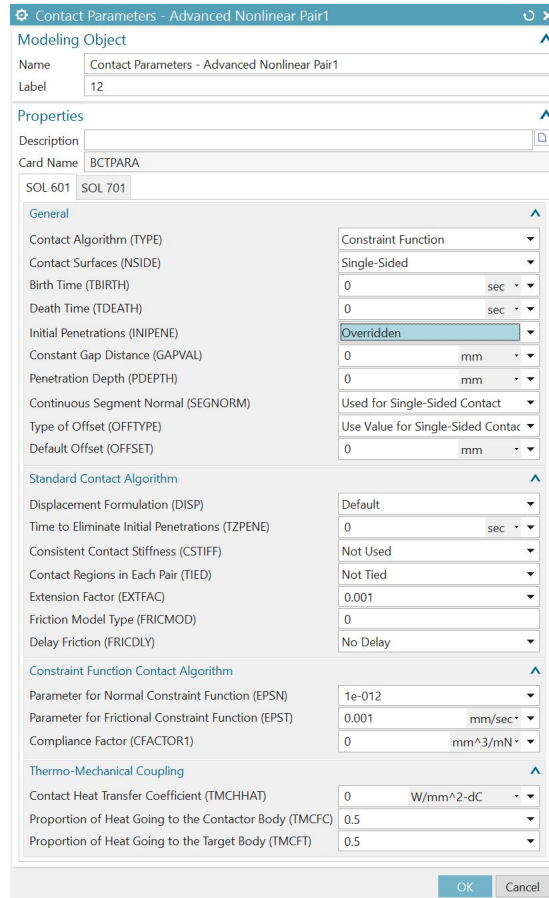


Figure 2.6: Advanced Nonlinear Contact Parameters

According to ADINA the constraint-function method is the most effective method in most cases and is also the default choice [8].

Initial Penetration

The initial penetration parameter's function is to deal with overlaps of nodes in the model. There are four options:

- **Eliminated** – initial penetration is eliminated, and the elimination time can be controlled.
- **Eliminated/Print penetrating nodes** – same as first option, but the penetrated nodes are listed and printed.

- **Ignored** – the initial penetrations are ignored, and the source nodes are allowed to penetrate target nodes.
- **Overridden** – the initial penetrations are overridden by values defined in the *Constant Gap Distance*.

Both the *Eliminated* and the *Overridden* option works well with surfaces that has interference or gaps. However, features involving curved meshes, e.g. shrink fit, ADINA suggests using the *Overridden* option and defining a gap value. This leads to more accurate results. Increased mesh density has the same effect [8].

Consistent Contact Stiffness

In order to account for additional stiffness contribution, introduced when the contact normal changes direction, the *Consistent Contact Stiffness* parameter can be turned on. Greater convergence rates can be achieved as a result.

Compliance Factor

Generally, the contact surfaces are assumed to be non-penetrable, which correspond to a compliance factor of 0. Nevertheless, a soft contact surface can be achieved by increasing the compliance factor, thus creating a compliant surface. The quantity of this factor typically lies in the order of $1e-8$ to $1e-5$ and can have a positive effect on the convergence rate. This option, however, is only available with the *constraint-function method*.

2.4 Simplified bearing model

As mentioned earlier, the connecting rod is connected to the crank shaft through a needle roller bearing, as seen in Figure 2.7. This bearing contributes to increased analysis complexity, as it consist of a total of 19 individual rolling elements. Using the complete model would demand an advanced model set up, as well as great computational power and time. Unnecessary complexity in the model should be avoided, assuming it does not have a major impact of the results. Therefore, a brief literature study was conducted

to get an overview of the different modelling techniques with the aim to simplify a needle roller bearing.

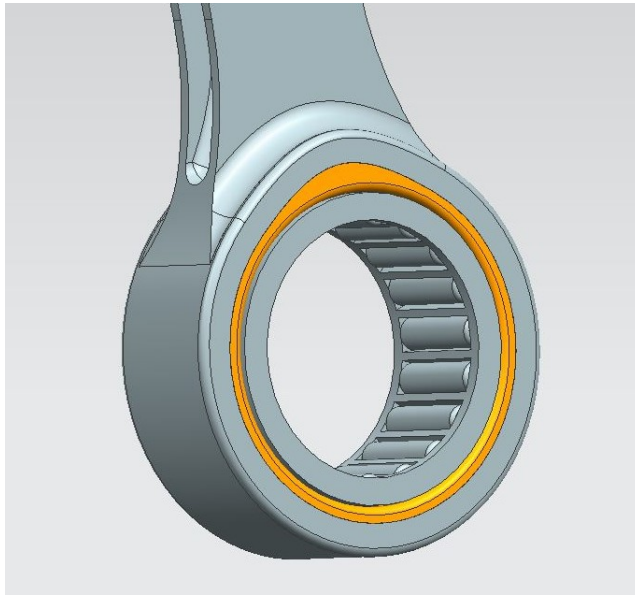


Figure 2.7: The needle roller bearing.

2.4.1 Previous work

There exist different studies and experiments on simplifying the FEM model of different types bearings. However, some of the most recent and applicable work, in the case of a simplified needle roller bearing, has been carried out by László Molnár et al (2010), Emil Claesson (2014) and Erik Adolfson (2015) [9][10][11]. Various different models were designed in these papers. They were tested in a Finite Element Analysis (FEA) and compared to a fully detailed needle roller bearing model. Those with the most promising results will now be presented:

The RBE3-ring model

The first model was developed by Erik Adolffsen and showed the most accurate results in his tests. The model consist of RBE3 elements connecting the outer surface of the shaft, to the inner surface of the bore. This allows for deformation between what is ef-

fectually the inner and outer ring of the bearing. However, it does not take into account the rolls impact on the inner surface.

The bush model

This model was one of two models suggested by Molnár et al in their research article for replacing the full needle roller bearing. It basically consist of a solid bush with the same thickness as the original bearing, as shown in Figure 2.8.

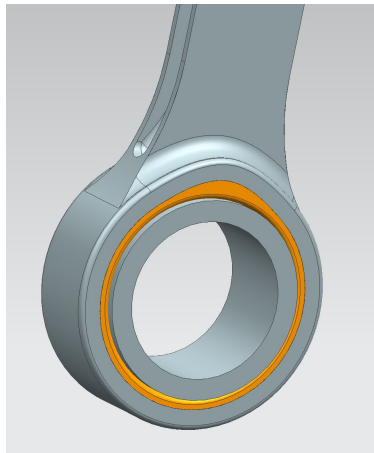


Figure 2.8: The bush replacement.

The intention is that the characteristics of the bush, e.g. the stiffness, is manipulated to be similar to the row of rolls in the bearing. Thus, producing equal amount of deformation as the the actual bearing.

The spring-element model

Both Claesson and Molnár et al have used this model as a substitute for the roller bearing. The essence of spring-element model is that each individual roll is substituted with a spring-element. The outer and inner ring is therefore connected through these springs. The stiffness of the rolls are calculated and assigned to each spring-element, thus controlling the deformation of each spring individually. This creates a more realistic representation of the overall stiffness. Figure 2.9 shows the general concept of this method [9]:

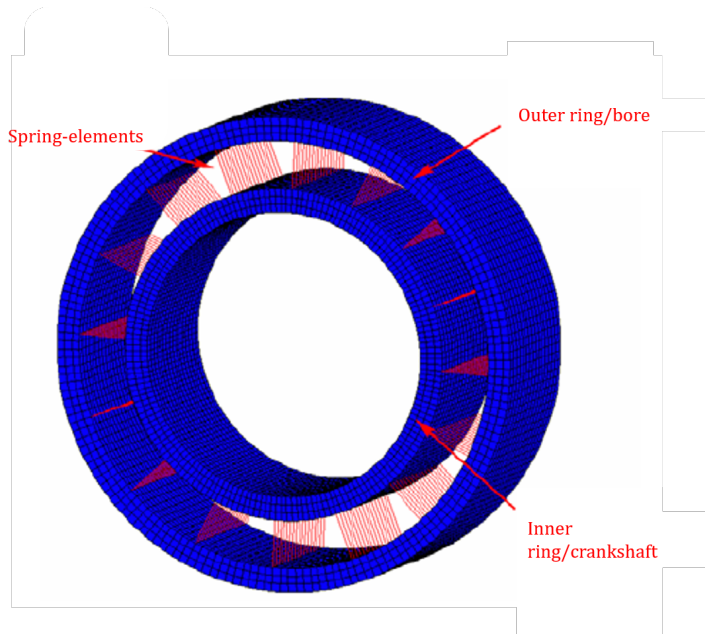


Figure 2.9: The spring-element model.

2.4.2 Comparison and selection of model

There are different pros and cons with each of the three models mentioned above. The spring-element and RBE3 model can result in unrealistic local stresses at their connections. On the other side, the bush-model does not account for the rolls interaction with the surface, and distributes the load evenly. However, the bush-model is simple to integrate in the structure of the connecting rod, as the other two models demands a more detailed modelling. The spring-model is considered to be the most accurate solution, as it opens up the opportunity to fine tune each individual spring (roll) to accurately represent the stiffness characteristic when subjected to various loads. Nevertheless, this feature is advantageous only in specific cases [9]. Therefore, considering the simplicity and accurate test results achieved by Molnár et al, it is reasoned that the bush-model is an appropriate substitution for the needle roller bearing. As concluded by Molnár et al:

"The FE data preparation work for bush model is simpler and provides adequate accuracy for practical examinations. Therefore substituting bush model with rough mesh is recommended for finite element modeling of common structures."

2.5 Calculation of bearing model characteristics

In order to construct a realistic replacement model of the needle roller bearing, material properties, e.g. the elasticity modulus, has to be modified to accurately represent the actual bearing.

An analytically approximation is performed to establish an appropriate Young's modulus for the new simplified bearing material. This approach includes calculating the ratio, α , between the two areas (original bearing and substituting bush). Since the Young's modulus is proportional to the area, this ratio is used to calculate the new and Young's modulus, representing the actual stiffness of the bearing (equation).

$$E_b = \alpha \times E_o \quad [MPa] \quad (2.1)$$

The cross sectional area of the two models are as follows:

Original bearing:

$$A_o = \pi r^2 \times n \quad [mm] \quad (2.2)$$

Where r is the roller radius and n is the number of rolls.

Substituting bush:

$$A_b = \pi(r_o^2 - r_i^2) \quad [mm] \quad (2.3)$$

Where r_o and r_i is the outer and inner radius of the bush respectively.

The ratio α can then be calculated as:

$$\alpha = \frac{A_o}{A_b} = \frac{\pi r^2 \times n}{\pi(r_o^2 - r_i^2)} = \frac{r^2 \times n}{r_o^2 - r_i^2} \quad (2.4)$$

Thus, equation 2.1 becomes:

$$E_b = \alpha \times E_o = \frac{r^2 \times n}{r_o^2 - r_i^2} \times E_o \quad [MPa] \quad (2.5)$$

Applying $r = 2mm$, $r_i = 15mm$, $r_o = 19mm$, $n = 19$ and for steel $E_o = 206\ 000$ MPa:

$$E_b = 115117.6 \text{ MPa} \tag{2.6}$$

This Young’s modulus is then used to modify the bearing material to represent the actual bearing stiffness, as shown in Figure 2.10.

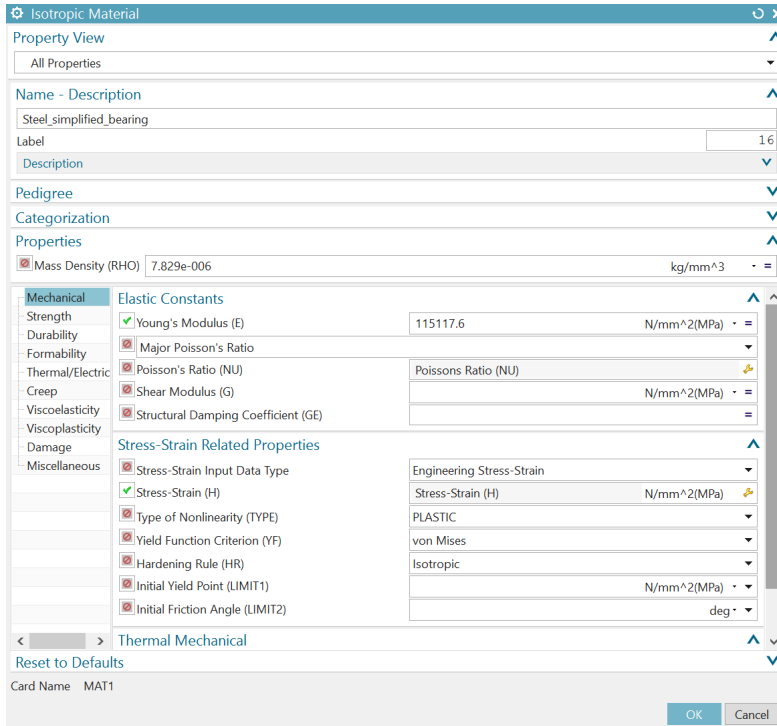


Figure 2.10: Modification of bearing material.

Chapter 3

Critical load cases and KPI's

In this chapter the identified load cases will be presented, as well as the defined *Key Performance Indicators* (KPI's).

3.1 Load Cases

There are mainly two load cases that are of interest when it comes to critical connecting rod loads and the cause of ovalisation:

- **Maximum combustion loads**
- **Maximum inertia loads**

The magnitude of these loads has been thoroughly investigated in the paper, *Dynamic Test Bench for Motocross Engines*, by Terje Rølvåg and Matteo Bella [12]. These values are extracted to be used in this analysis. The two interference fits also leads to loads in the small and big ends, as shown in Figure 3.1. These are accounted for in the analysis set up.

3.1.1 Load Case 1: Maximum combustion loads

At low engine speed, defined as less then 9000 rpms, the peak piston pressure occurs. This leads to the maximum compression force acting on the connecting rod. The magnitude of this compression force is in the order of **50 kN** [12] and usually appears 10-13

degrees ATDC (After Top Dead Center). However, for the simplicity of the analysis, the horizontal force component this involves is neglected. Figure 3.1 shows how the forces are acting on the connecting rod.

3.1.2 Load Case 2: Maximum inertia loads

The second load case is due to the inertia effects acting on the connecting rod. These forces occur at higher speeds, usually above 1400 rpms, and generates tension of the connecting rod. The inertia forces are initiated by the rotating crank shaft, as well as the reciprocating masses of the piston, piston pin and the rod itself. These tension forces are about **10 kN**, according to [12], and are in some cases the leading cause of failure, rather than the combustion loads.

3.2 Key Performance Indicators

In order to quantify the ovalisation of the big and small end, as well as bench marking the difference of simulation method (solver), Key Point Indicators (KPI's) were defined. They aim to capture the integrity of the connecting rod, both related to displacement and stress/pressure. The selected KPI's are listed below:

1. Maximum Big End deformation
2. Maximum Small End deformation
3. Big End contact pressure
4. Small End contact pressure
5. Maximum Connecting Rod Von Mises Stresses
6. Small End to beam transition

KPI 1 and 2 will be quantified by studying displacement graphs of the two bores and compared between the two solvers. KPI 3 and 4 is investigated by looking at contact pressure output, for the specific regions. The last KPI, number five, is intended to strengthen the accuracy and foundation of comparing the two solvers.

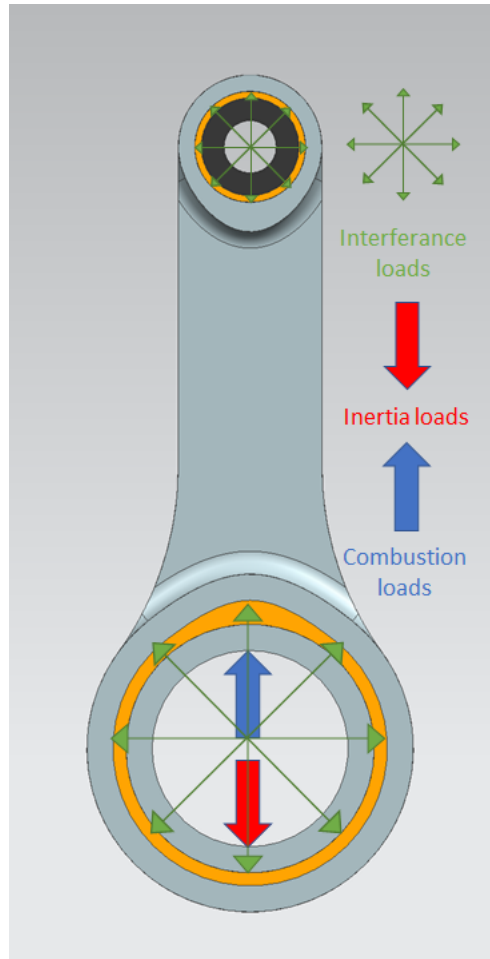


Figure 3.1: Forces acting on the connecting rod.

Chapter 4

Model description

The connecting rod used in this thesis is a H-profiled titanium rod, with an insert in each end. A titanium piston pin is attached to the small end, and the simplified bearing model is attached to the big end. Figure 4.1 shows the model configuration.

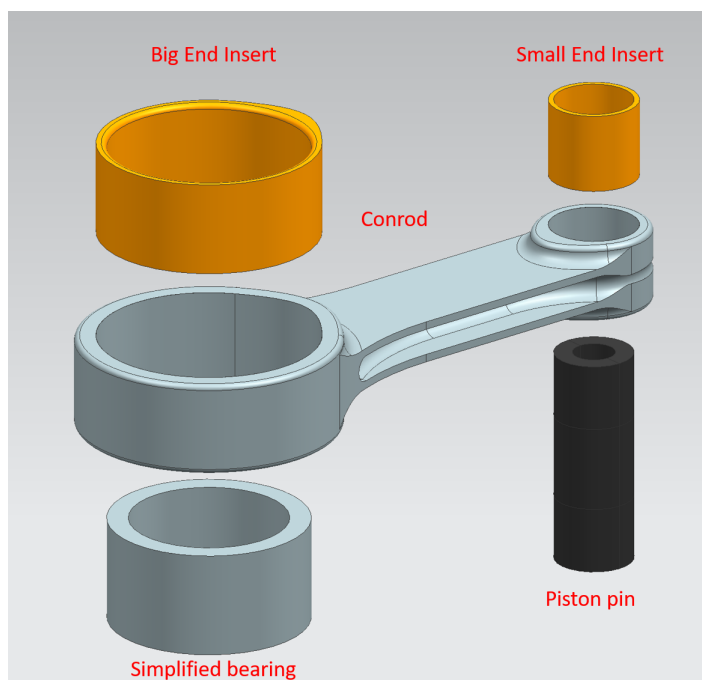


Figure 4.1: The five parts of the conrod.

The model has been slightly simplified by removing the outside edge blends on the big and small ends, as well as the edge blend on the big end insert. This was done by using the *Synchronous Modelling* command *Delete face*. This simplification contributes to a less complex finite element model, thus reducing the solution time.

4.1 Contact characteristics

The manufacture of the connecting rod at hand, MXRR, provided the necessary data of the contact characteristics to accurately describe the model. The two inserts is press-fitted with an interference of **0.03 mm** each (contact pair 1 and 3). The contact pairs 2 and 4 has a play of **0.025 mm** and **0.01 mm**, and a *Coefficient of Static Friction* of **0.1** and **0.4**, respectively.

This model consist of a total of four surface pairs in contact, as listed below:

1. Small End Bore - Small End insert outer
2. Small End insert inner - Piston pin
3. Big End bore - Big End insert outer
4. Big End insert inner - Bearing outer

4.2 Materials

The materials and material properties used in this connecting rod are provided by the manufacturer, except from the simplified bearing material. The properties are defined to be nonlinear, which is necessary for these simulations. The applied materials are described in Table 4.1:

Material	Part	Young's Modulus [MPa]	Poisson's Ratio	Mass Density [kg/mm³]	Yield Strength [MPa]	Ultimate Tensile Strength [MPa]
Titanium	Conrod and Piston Pin	110 000	0.34	4.43e-6	862	1065
Steel 1	Big and Small End Inserts	206 000	0.3	7.7e-6	235	340
Steel 2	Bearing	115 118	0.3	7.7e-6	235	340

Table 4.1: Material composition.

Chapter 5

Finite Element Model

5.1 Mesh Mating

In order to increase the precision of the results, the tool *Mesh Mating - Free Coincident Condition*, was used on the surfaces in contact. This aligns the nodes of the different bodies and creates a continuous mesh, without any connections between them. The contacting faces were manually selected for the mesh mating, as it was discovered that some irregularities and distortion of the mesh occurred when this was done automatically, as seen in the figure below (Figure 5.1)

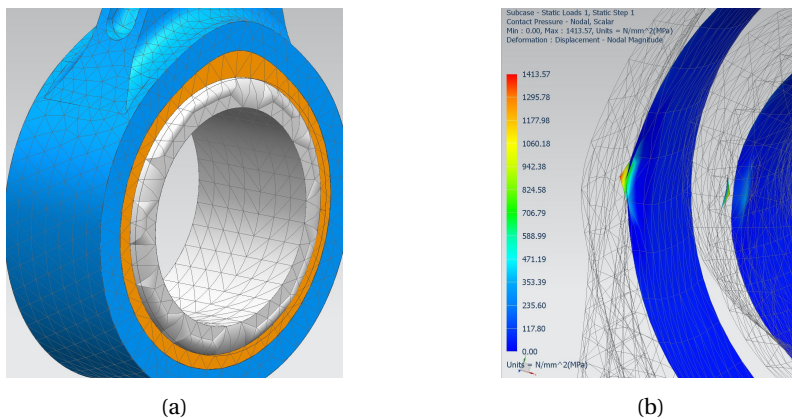


Figure 5.1: Distortion of mesh (a) and face contact irregularity (b).

5.2 Meshing

In order to achieve accurate results in the simulation, it is essential that the finite element model is well prepared, with the appropriate element size and connectors. A too rough mesh, will result in inaccuracies in the results. On the other side, an overly fine mesh could result in dramatically increased CPU time without corresponding increased accuracy. Therefore, the selection of the correct element size should be carefully inspected. Also, the element type should be chosen to best capture the natural shape of the model, and avoid the appearance of distorted elements.

The connecting rod has some sharp edges other complex geometry that would be difficult to capture with the CHEXA elements. The CTETRA element is the common choice for these kind of structures, and was deemed fitted for the connecting rod as well. Some parts of the model, such as the two inserts and the simplified bearing, could be accurately swept meshed with CHEXA elements. However, in a contact analysis it is preferable to use same element types on faces/bodies in contact, in order to achieve continuous non-distorted mesh.

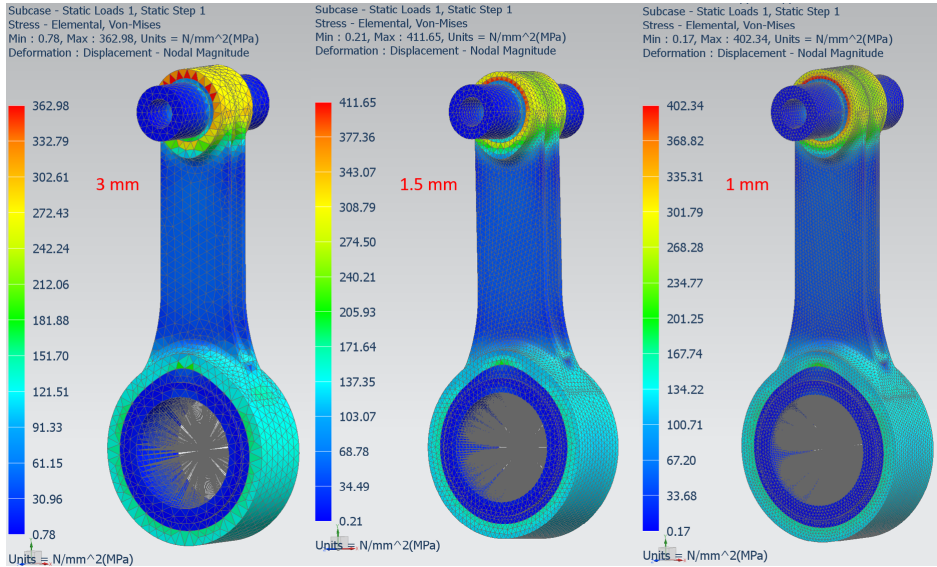


Figure 5.2: Convergence analysis.

To establish the optimal element size, three linear static simulation was conducted, with the respective element sizes of 3mm, 1.5mm and 1mm, with the intention to investigate convergence in the results. The *Max Von Mises Stresses* output was selected as convergence reference. Figure 5.2 shows the results of the simulations and in Table 5.1 the different results are compared.

Element Size [mm]	Max Von Mises Stress [MPa]	CPU time
3	363	2 min
1.5	412	20 min
1	402	1 h 30 min

Table 5.1: Convergence analysis.

It is evident from the figure, as well as Table 5.1, that average element size of 1.5 mm is the optimal mesh density. Further refinement would only lead to increased analysis complexity and CPU time. This correlates good with results found in similar analysis done by A.Londhe et al (2009) in the papaer *Finite Element Analysis of Connecting Rod and Correlation with Test*, where an element size of 1.5 mm where used as well [13].

The mesh quality was also checked by enabling *Strain Output Request*. This creates an analysis quality report which can be accessed after the simulation. The 1.5 mm element model corresponded to a confidence level based in energy norm of 97.39%, which is considered to be high. Everything above 95% is according to NX acceptable and does not require further refinement. The entire model was therefore meshed with CTETRA elements with 1.5 mm average element size, which resulted in a total element count of **93 183** . The complete FE model is seen in Figure 5.3.

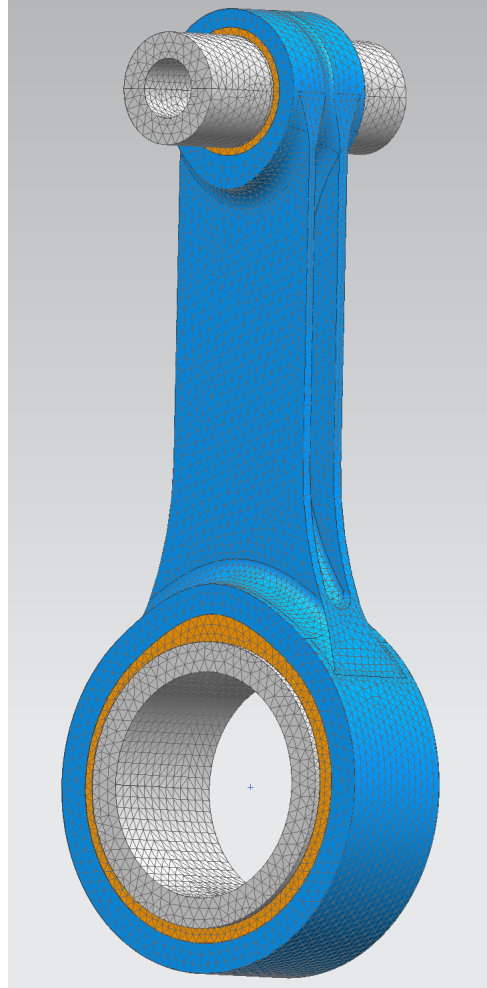


Figure 5.3: The FE model

5.3 RBE2 connection

As a step to further simplify the model, the crank shaft has not been modelled. This part is assumed to be much stiffer than the rest of the model, and are therefore replaced with a RBE2 element. The master node is located in the center of the big end, and the slave nodes are attached to the inner face of the simplified bearing, as seen in Figure 5.4.

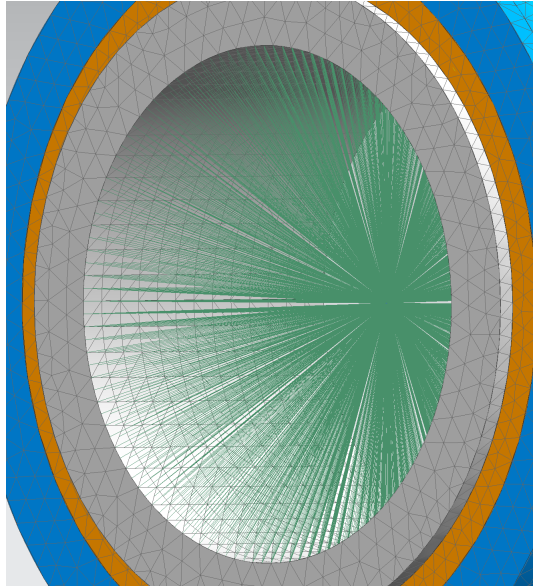


Figure 5.4: The RBE2 element replacing the crank shaft.

The RBE2 element creates a rigid connection at the inside of the bearing. The intention is to apply the compression and tension loads in the master node. This will drastically reduce the complexity of the model, in comparison to using a fully modelled crank shaft. Nonetheless, the increased stiffness should be accounted for when analyzing the results.

5.4 Nodal Coordinate System

In order to capture the ovality of both the small and big end, it is essential that the solver writes the nodal displacements of these features. This is possible by assigning a cylindrical *Nodal Displacement Coordinate Systems* at the inner radius of each end. Cylindrical coordinates consists of three parameters: radius, theta and z, as illustrated in Figure 5.5.

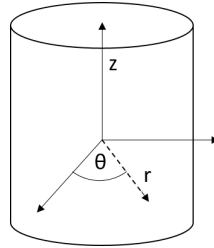


Figure 5.5: Cylindrical coordinate system.

The displacement in the r -direction will therefore represent the deformation of the big and small end respectively, and can give a good indication of the ovalisation of the bores. Figure 5.6 shows where the respective nodal displacement coordinate systems are assigned.

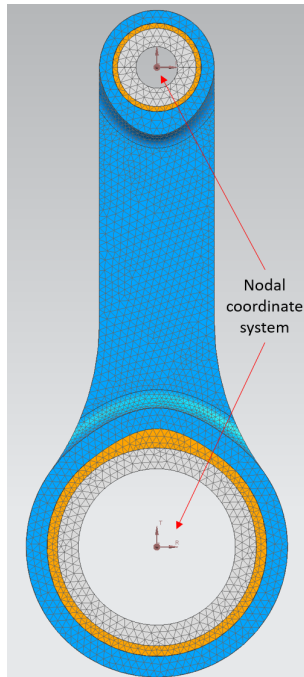


Figure 5.6: The two assigned nodal coordinate systems.

Chapter 6

Finite Element Analysis

As mentioned earlier, there are commonly two solvers in NX which are used for solving contact problems: SOL 101 and SOL601. The approach and results of using these two solvers will now be presented. It is assumed that the SOL 601 solver will have the highest accuracy.

6.1 SOL 101

As described in the previous chapter, SOL 101 is a linear static solver. However, it has the ability to solve nonlinear problems, such as contact. There are limited options for contact parameters, but interference and play is possible to achieve.

6.1.1 Boundary Conditions

The boundary conditions of the simulation set-up includes: constraints, loads and simulations objects (contact condition). To accurately and systematically assign both constraints and contact conditions, *regions* where defined to the model. These regions includes the inner/outer faces of the inserts, bores and piston pin.

Constraints

The model is fully constrained, as seen in Figure 6.1, at the regions of the piston pin which are in contact with the piston bosses in a engine. This is to ensure a stable model,

while still achieve an accurate simulation method.

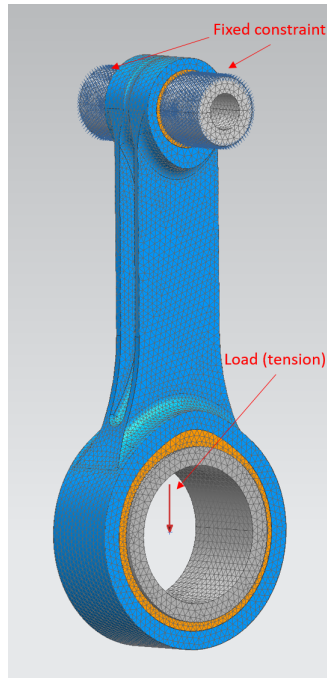


Figure 6.1: Constraints and load applied to the model (Load Case 2, displayed without the RBE2 element for convenience).

Loads

The loads are applied at the master node of the RBE2 element attached to the bearing, as seen in Figure 6.1. Corresponding to the load cases 1 and 2, the loads are defined in the positive and negative y-direction in the global coordinate system. The loads are, as mention earlier, 50 000 and 10 000 Newtons for the two loads cases respectively.

Simulation Objects - Surface-to-Surface Contact

As described in 4, there are four contact pairs in this model. Each individual contact surface are defined as a region, in order to manually control the contact condition. As the contact conditions are unique for each contact pair, manually assigning them gives a better control of the contact formulations. Figure 6.2 shows the defined parameters of contact pair 1 (Small End bore - Small End insert). The two contact pairs are selected,

and a *Coefficient of Static Friction* is entered. Both contact pair 1 and 3 are assigned with a somewhat arbitrary COF of **0.5**, which are a typical value for such contact. This COF is mostly intended to stabilize the model. Generally, the source region should be assigned to the body with the smallest element size [4]. In this case however, the entire model is meshed with the same element size and therefore the correct definition of source/target region is not of interest. Figure 6.2 shows how the interference is accounted for by expanding the region *SE Bore* by 0.03 mm. This offsets the region by the defined value, creating a initial penetration in the other region in the contact pair, *SE insert outer*.

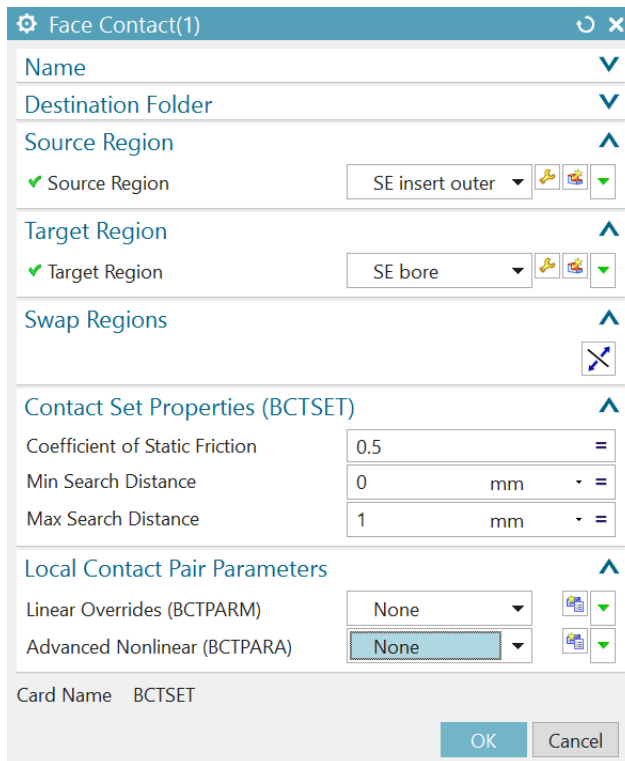


Figure 6.2: Surface-to-Surface Contact condition.

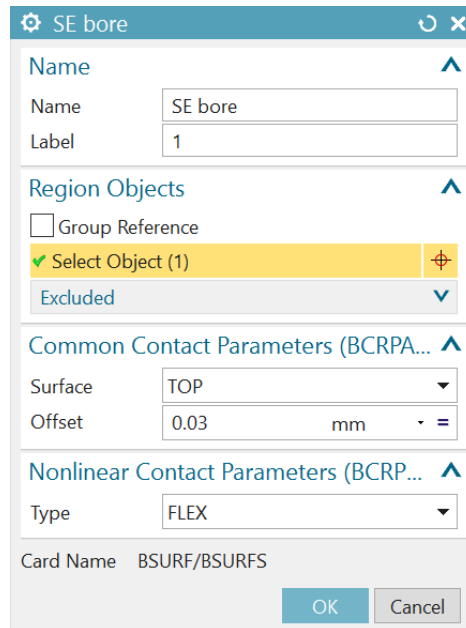


Figure 6.3: Contact parameter - 0.03 mm offset.

6.2 SOL 601

The other simulation method used to capture the ovalisation of the connecting rod, is by using the nonlinear solver SOL 601. This is an advanced nonlinear solver, capable to define even more specific contact parameters.

6.2.1 Boundary Conditions

When proceeding from the SOL 101 solver to SOL 601, the same boundary conditions can be used in the SOL 601 simulation set up. However, some modifications will increase the accuracy, as well as the convergence rate of the solution process, and are recommended to implement.

Constraints

The constraints are the exact same as for the SOL 101 simulation, and are just dragged into the SOL 601 simulation set up.

Loads

The loads are the same as in the SOL 101 simulation, but are gradually applied over time. Since the loads are relative large, especially for the compression (50 kN), gradually applying the load assure convergence of the simulation and general stability. This is done by defining a field of time-vs-load values, instead of a constant value. For this analysis, a linear curve from (0,0) to (50, 50 000) was defined for the compression load case, as seen in Figure 6.4. Similar curve was for the tension load case, only with 10 000 as end point for the load.

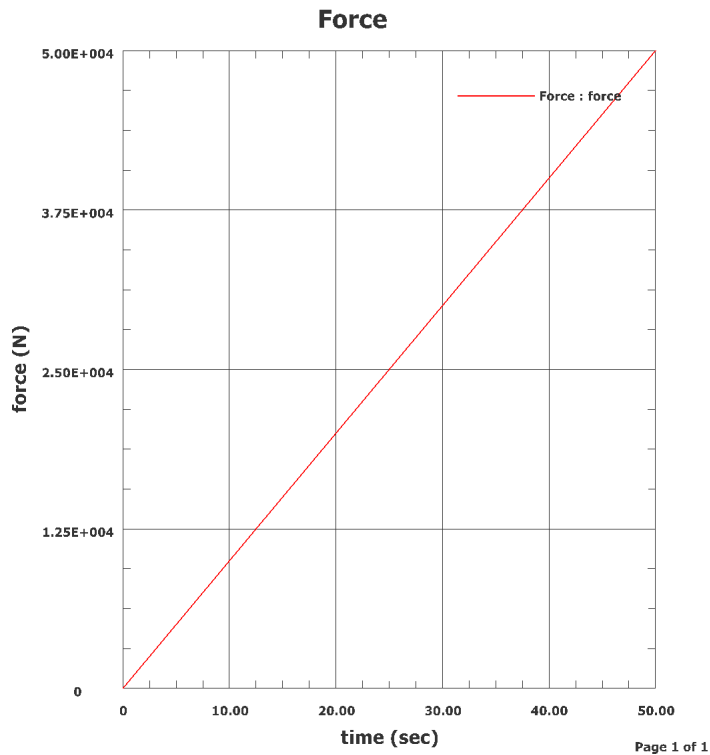


Figure 6.4: Load vs time curve for Load Case 1.

The exact values of this curve is more or less arbitrary, as it is the time stepping that control the actual rate of the applied load. They are mostly chosen for conveniences sake.

6.2.2 Time Step Interval

By default, the SOL 601 solver operates with a single time step of 1 second. This can be changed in the solution dialog, under *Case Control*. For the compression analysis it was chosen a number of 100 time steps with an increment of 0.5 seconds (resulting in 50 seconds in total). As for the tension analysis, 50 times steps, with corresponding 1 second incrimination was considered to be enough for applying the load, as seen in Figure 6.5 . It was observed that especially in the first time steps, it is crucial to have small loads involved to achieve a stable model.

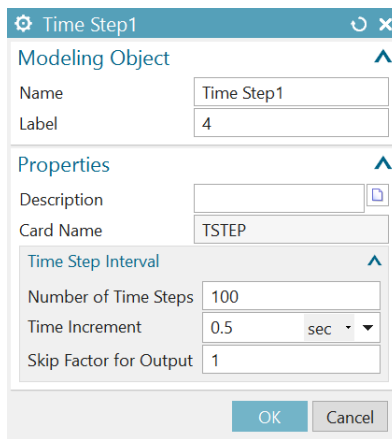


Figure 6.5: The time stepping of the solution.

The selection of time increment is based partly on similar cases found in the literature, as well as a trial-and-error approach to this specific problem. Finding the absolute optimal time incrimination was considered to be unnecessary use of time, as the *Strategy Parameter, Automatic Time Stepping* (explained below), automatically control the time stepping to ensure convergence of the analysis.

6.2.3 Strategy Parameters

The strategy parameters defines parameters for solution strategy and control. The default parameters are appropriate for most structural analyses. Nonetheless, some parameters has been tweaked for this analysis. The *Automatic Time Stepping* is chosen as the *Automatic Incrimination Scheme*, shown in Figure 6.6. This reduces the simulation time, as the solver creates it own time steps. The ATS adjusts the time steps to achieve

convergence of the simulation. These steps are larger if the solution converges, and smaller if convergence is not reached. However, the predefined time steps has to be within a reasonable size, as the ATS does not perform unlimited reduction of time steps. Maximum iterations are changed from 15 to 25 iterations, to achieve convergence.

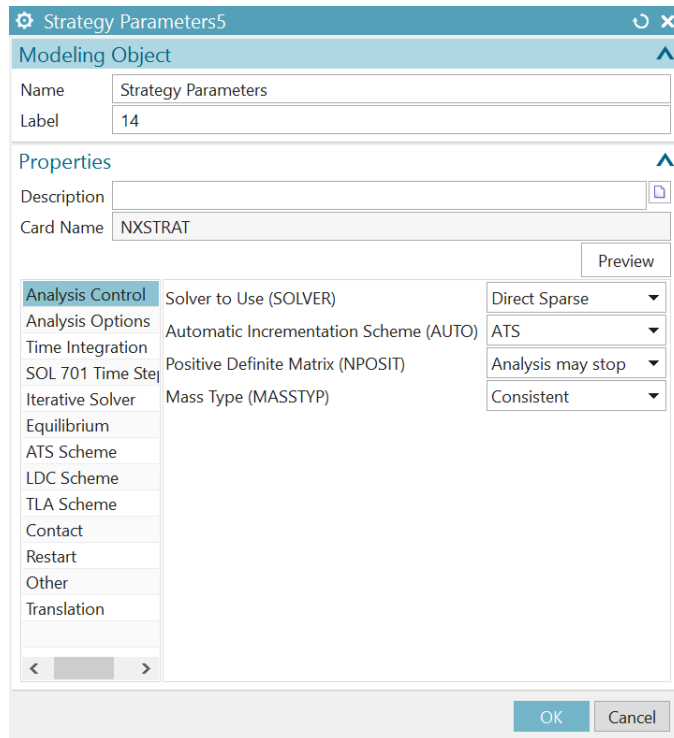


Figure 6.6: Strategy parameters.

6.2.4 Simulation Objects - Surface-to-Surface Contact

The surface-to-surface contact condition are assigned the same way as in SOL 101. The region offset is however set to 0, as the interference/play are rather defined in the non-linear contact parameters. This is assumed to be more accurate, as explained earlier, for shrink fit analyses and curved mesh. Further, nonlinear contact parameters are defined. The interference value of 0.03 mm are entered and *Consistent Contact Stiffness* is selected, among other parameters. An overview of the parameters used in Contact Pair 1 is shown in Figure 6.7.

Properties ▲

Description

Card Name BCTPARA

SOL 601 SOL 701

General ▲

Contact Algorithm (TYPE)	Constraint Function
Contact Surfaces (NSIDE)	Single-Sided
Birth Time (TBIRTH)	0 sec
Death Time (TDEATH)	0 sec
Initial Penetrations (INIPENE)	Overridden
Constant Gap Distance (GAPVAL)	-0.03 mm
Penetration Depth (PDEPTH)	0 mm
Continuous Segment Normal (SEGNORM)	Used for Single-Sided Contact
Type of Offset (OFFTYPE)	Use Value for Single-Sided Contact
Default Offset (OFFSET)	0 mm

Standard Contact Algorithm ▲

Displacement Formulation (DISP)	Small Displacement
Time to Eliminate Initial Penetrations (TZPENE)	0 sec
Consistent Contact Stiffness (CSTIFF)	Used
Contact Regions in Each Pair (TIED)	Not Tied
Extension Factor (EXTFAC)	0.001
Friction Model Type (FRICMOD)	0
Delay Friction (FRICDLY)	No Delay

Constraint Function Contact Algorithm ▲

Parameter for Normal Constraint Function (EPSN)	1e-012
Parameter for Frictional Constraint Function (EPST)	0.001 mm/sec
Compliance Factor (CFACOR1)	1e-008 mm ³ /mN

Thermo-Mechanical Coupling ▲

Contact Heat Transfer Coefficient (TMCHHAT)	0 W/mm ² -dC
Proportion of Heat Going to the Contactor Body (TMCFC)	0.5
Proportion of Heat Going to the Target Body (TMCFT)	0.5

Figure 6.7: Nonlinear contact parameters.

6.3 FEA results

There where in total performed four analyses; LC 1 and 2 for SOL 101 and SOL 601, with the intention to capture the ovalisation of the two ends of the connecting rod. In order to accurately analyze the ovalisation, it was created graphs of the displacements in the big and small end bores respectively. The displacements are by default set relative to the global coordinate system. To get the displacements relative to the two cylindrical nodal displacement coordinate systems created, the *Post View* had to be edited, as seen in the Figure 6.8, this was done by selecting the appropriate coordinate system and defining R (radius) as the displacement parameter.

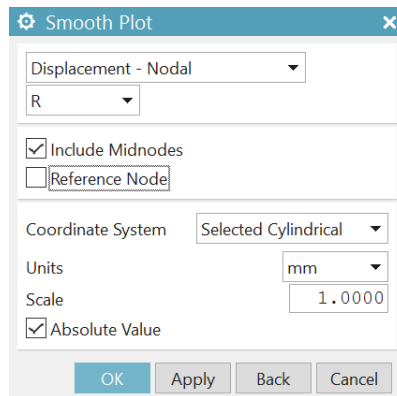


Figure 6.8: Post View modification.

Then the graph can be created to correspond to the displacements in the bores. The parameter θ was chosen as variable parameter, thus plotting the displacement around the face of the bore. Figure 6.9 shows how the graph is defined and Figure 6.10 shows values of θ relative to the model.

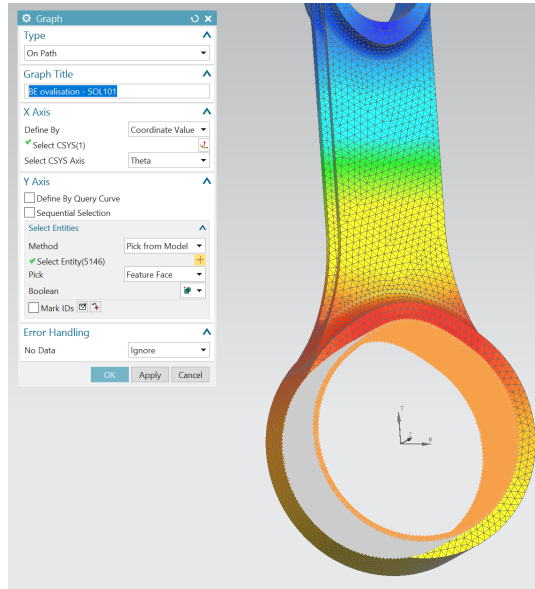


Figure 6.9: Creation of displacement graph of the big end bore.

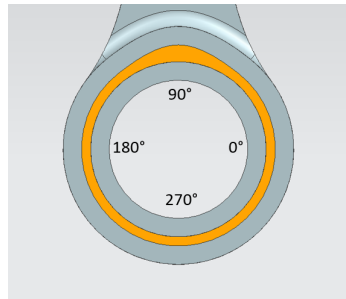


Figure 6.10: Theta values around the big end (similar for the small end).

6.3.1 SOL 101

Load Case 1 - Compression

As mentioned, load case 1 involves a 50 kN compression force acting on the connecting rod from the bearing. The simulation time was approximately **25 minutes**. Figure 6.11 and 6.12 shows the ovalisation graphs of the big and small end respectively, for the SOL 101 solver under compression.

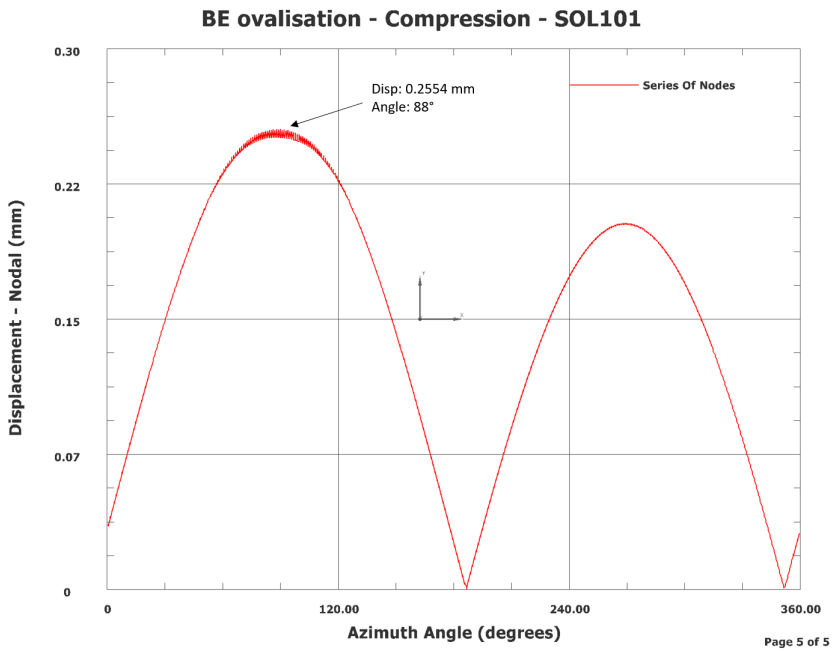


Figure 6.11: Displacement graph of the big end ovalisation under compression - SOL 101.

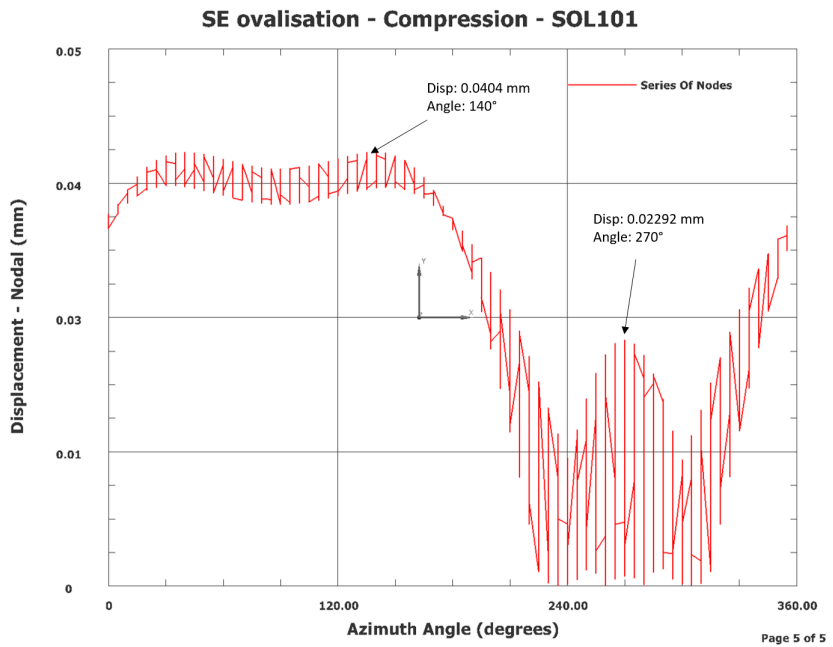


Figure 6.12: Displacement graph of the small end ovalisation under compression - SOL 101.

As seen from the figures, the maximum deformation of the big end occurs at approximately **90 degrees** from the x-axis, with a magnitude of **0.255 mm**. A similar peak can be observed at 270 degrees, as seen in the graph. These values are absolute, and the two deformation peaks are actually in opposite direction.

For the small end, the largest deformation appears at the range from 0 to about 160 degrees, with a peak of **0.0404 mm** at **140 degrees**. Another peak is prominent at **270 degrees**. These results are more scattered due to a lower number of nodes at the face of the Small End bore.

Figure 6.13 shows the contact pressure and the Von Mises stresses. Its evident from the figure that the edge effect can be observed in the small end, and contributes to large stress concentration. At the big end, the highest contact pressure occurs at the top of the oval insert, at a magnitude of **280 MP**. Another highly stressed area of the connecting rod can be seen at the transition from the beam to the small end, as shown in Figure 6.14.

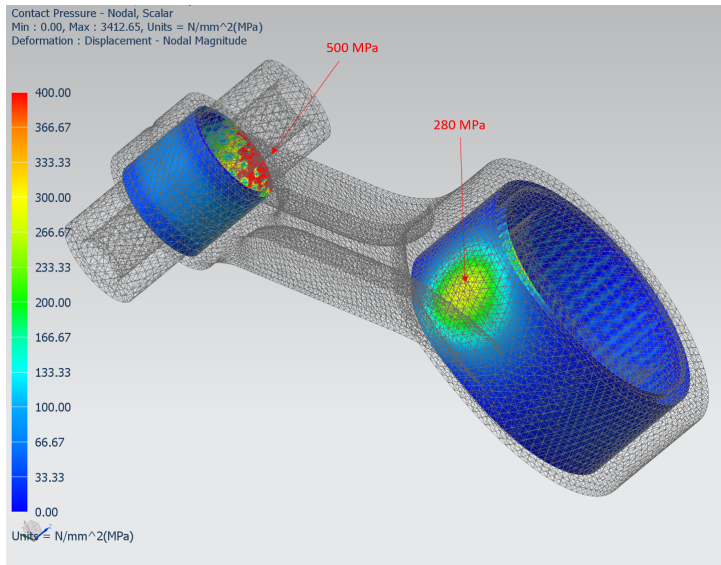


Figure 6.13: Contact pressure (KPI 3 and 4) under compression - SOL 101.

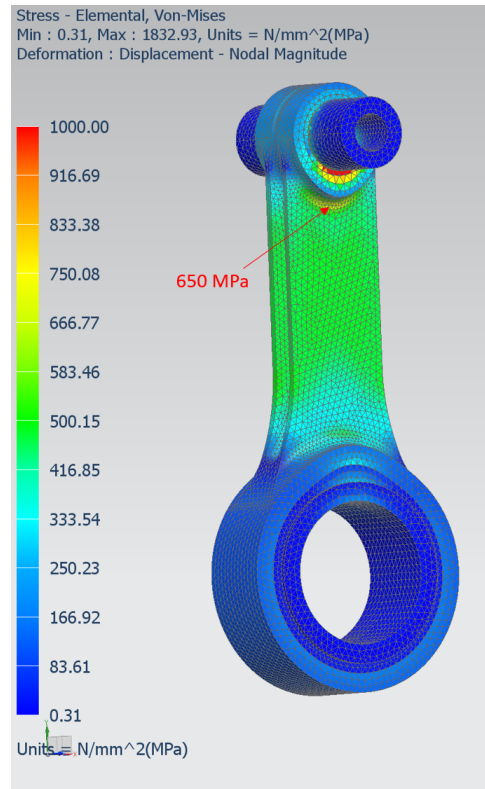


Figure 6.14: Von Mises stresses (KPI 5 and 6) under compression - SOL 101.

Load Case 2 - Tension

Load Case 2, with 10 kN tension force, where solved after **20 minutes** using the SOL 101 solver. Figure 6.15 and 6.16 shows the corresponding deformation graphs of the two bores in the connecting rod.

In tension, the big end deformation is most prominent at **312 degrees** with a magnitude of **0.1661 mm**. A peak can also be observed at around 130 degrees, just above 0.1 mm. In the case of the small end, there are not so much ovalisation occurring. Just a small peak at **270 degrees** with a deformation of **0.0326 mm**, barely above the interference value of 0.03 mm.

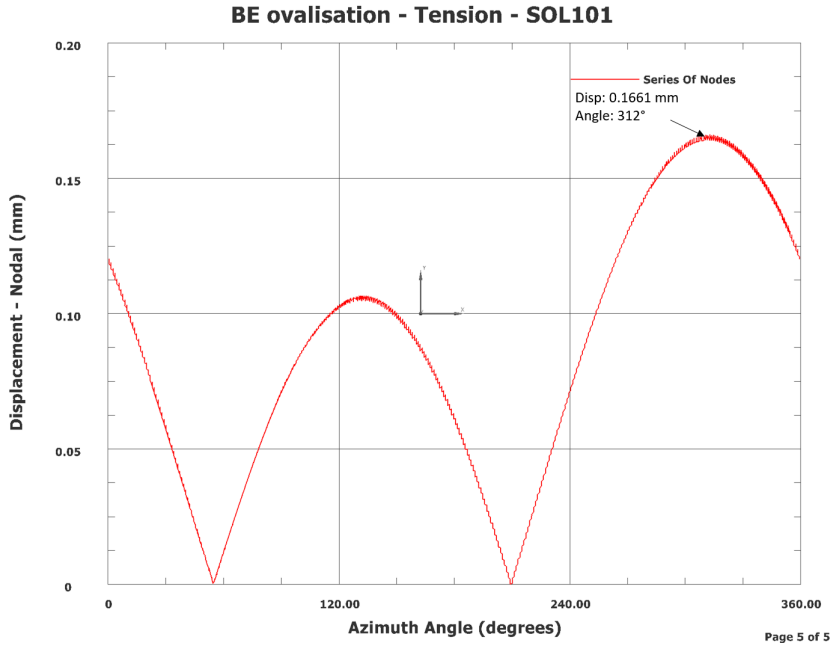


Figure 6.15: Displacement graph of the small end ovalisation under tension - SOL 101.

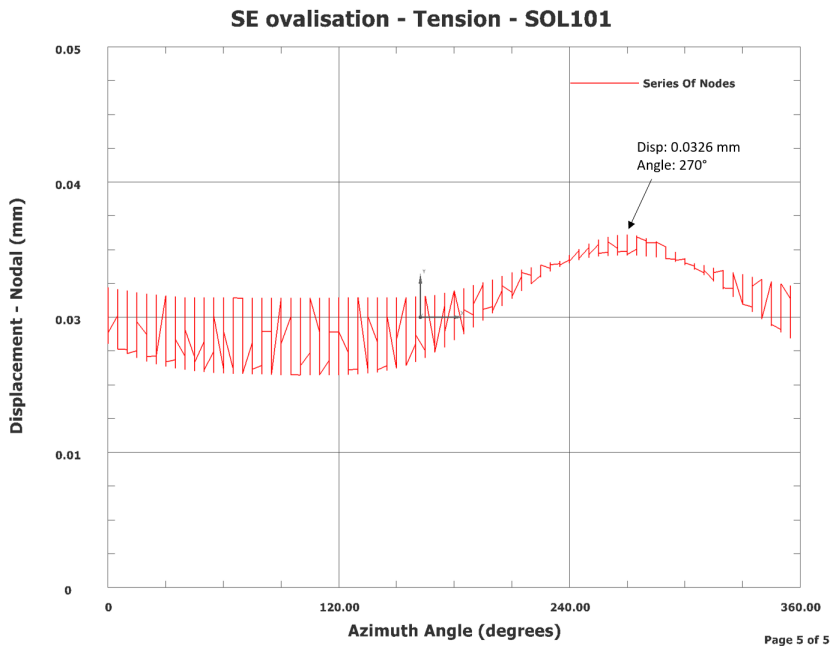


Figure 6.16: Displacement graph of the small end ovalisation under tension - SOL 101.

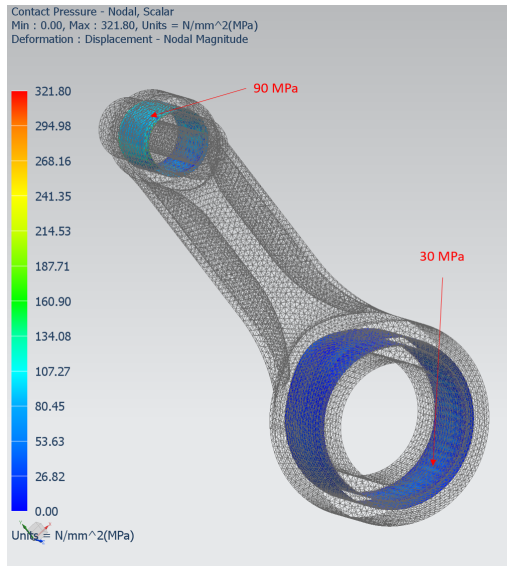


Figure 6.17: Contact pressure (KPI 3 and 4) - SOL 101.

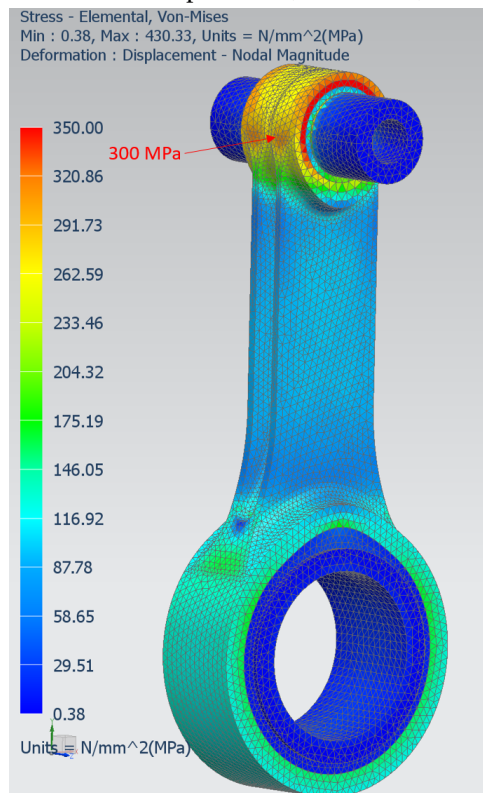


Figure 6.18: Von Mises stresses (KPI 5 and 6) - SOL 101.

Figure 6.17 shows the contact pressure, with a Small End contact pressure of **90 MPa** and **30 Mpa** in the big end. The stress plot from Figure 6.18 shows a highly stressed region around the small end (above 350 MPa), as well as on the side in the transition to the beam (300 MPa). The big end is subjected to an evenly distributed stress field of about **140 MPa**.

6.3.2 SOL 601

Load Case 1 - Compression

The compression analysis in the SOL 601 solver was completed after a solution time of 5 hours. It took about 150 iterations to reach convergence of all time steps.

It can be seen from Figure 6.19 that the big end ovalisation happens in the longitudinal direction of the connecting rod. At **90** and **270 degrees**, the deformation is **0.2618 mm**. The same can be seen at the small end, however with the biggest deformation of **0.0630 mm** at **270 degrees**, being the bottom of the Small End (Figure 6.20). A peak can also be seen at **90 degrees**.

Figure 6.21 displays the contact pressure, with a maximum value of **400 MPa** at the small end edge, and a field at the big end top of **180 MPa**. From Figure 6.22 the edge effect is causing highly stressed areas at the small end edge. Also, at the transition to the beam, it shows a stress concentration of **570 MPa**.

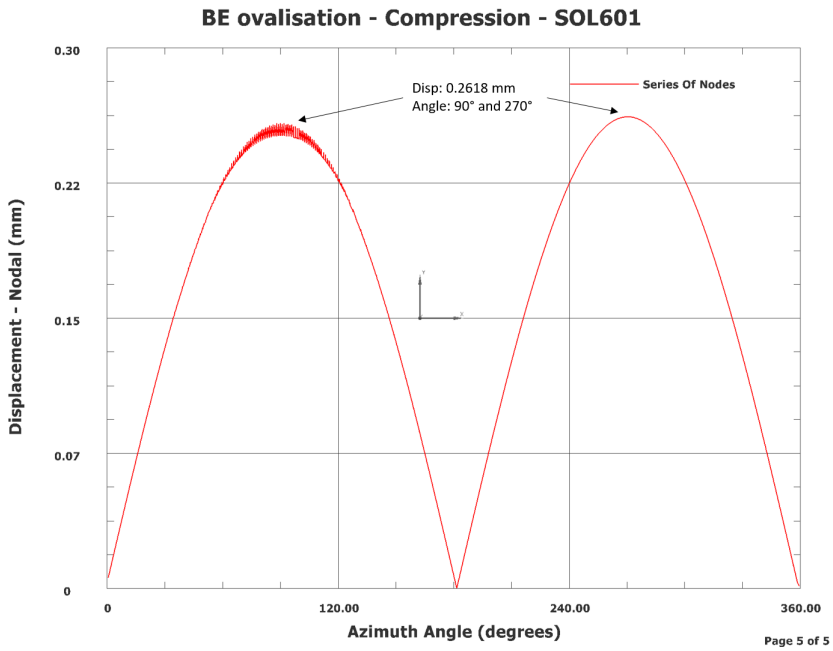


Figure 6.19: Displacement graph of the big end ovalisation under compression - SOL 601.

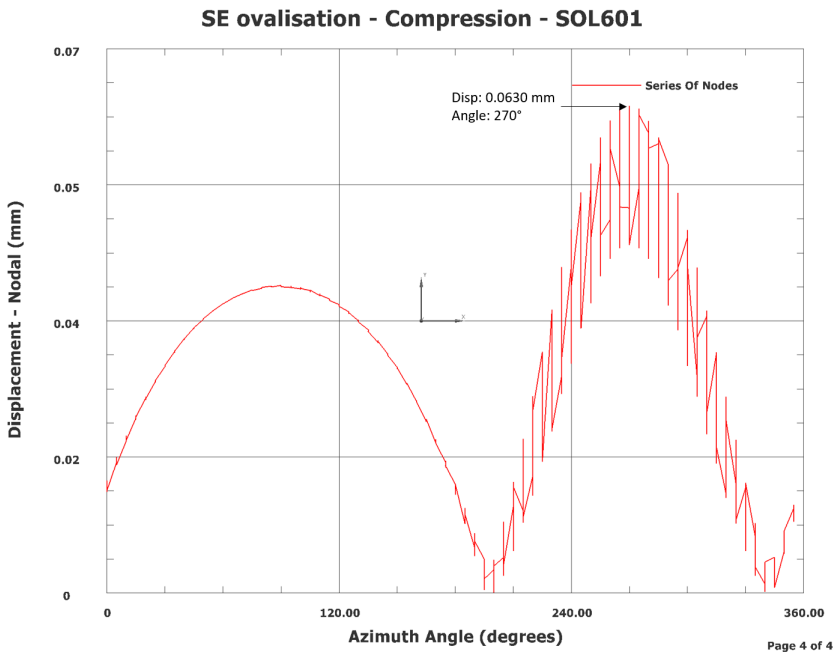


Figure 6.20: Displacement graph of the small end ovalisation under compression - SOL 601.

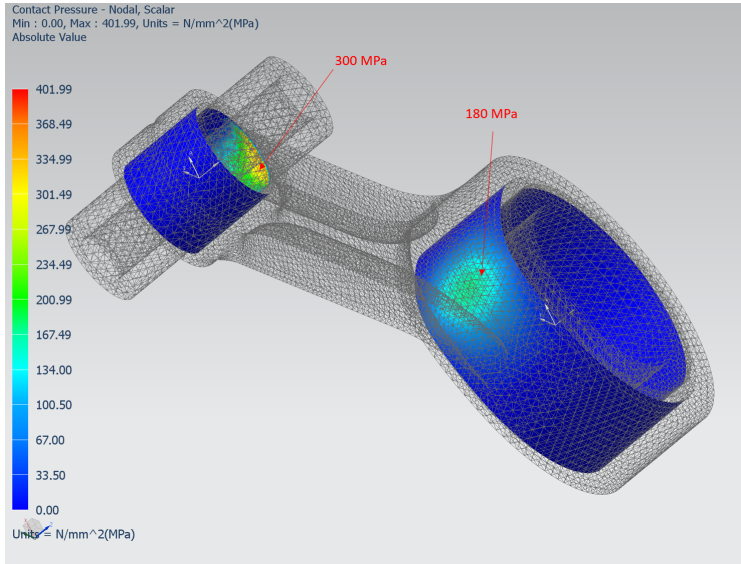


Figure 6.21: Contact pressure (KPI 3 and 4) - SOL 601.

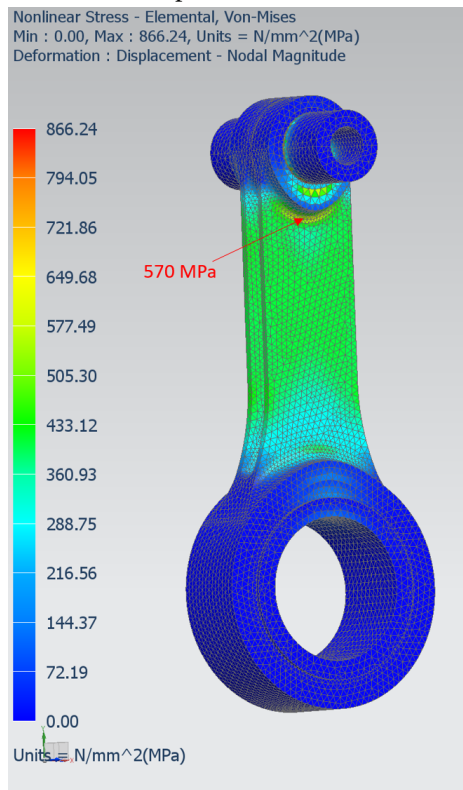


Figure 6.22: Von Mises stresses (KPI 5 and 6) - SOL 601.

Load Case 2 - Tension

The solution time of the SOL 601 analysis of LC 2 was 3 hours. Approximately 100 iterations were performed.

Figure 6.23 and 6.24 shows the resulting graphs created. Similar as previous big end graphs, its at **270 degrees** the largest deformation occurs, with a magnitude of **0.1432 mm**. A uniform peak can be seen from 30 to 150 degrees. The small end graph also shows a peak at **270 degrees** and a displacement of **0.0468 mm**. No other noticeable deformation else in the small end bore can be observed.

As seen from Figure 6.25, the Small and Big End contact pressure is about **70** and **30 MPa**, respectively. Figure 6.26 shows that there are several areas of stress concentrations prominent in the body. The outside of the beam transition, is such an area, as well as the top/side area of the big end bore.

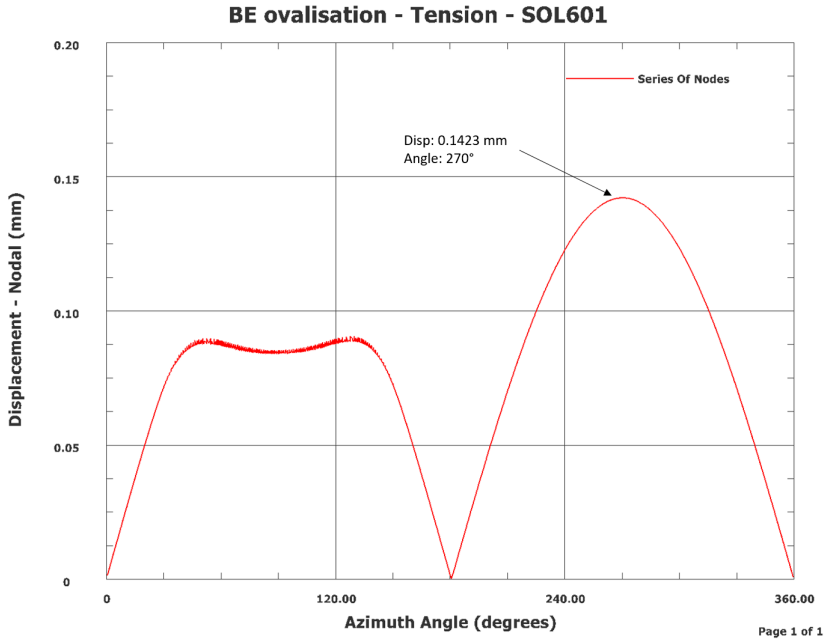


Figure 6.23: Displacement graph of the big end ovalisation under tension - SOL 601.

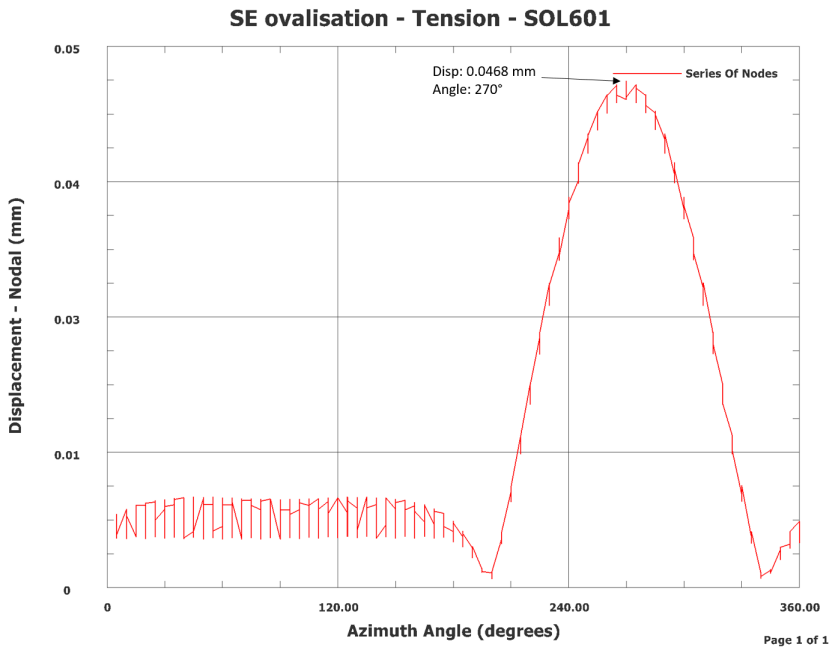


Figure 6.24: Displacement graph of the small end ovalisation under tension - SOL 601.

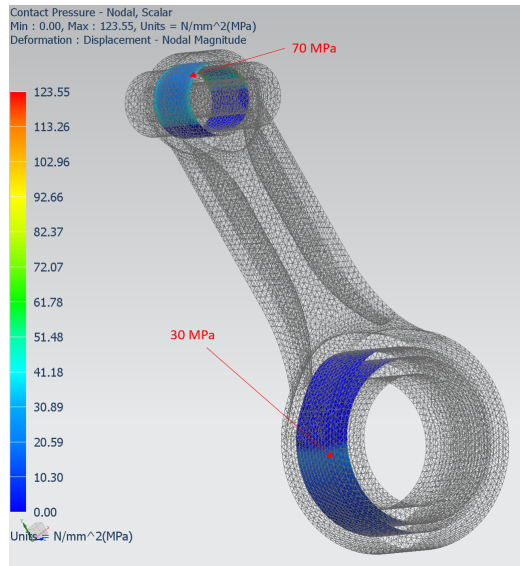


Figure 6.25: Contact pressure (KPI 3 and 4) - SOL 601.

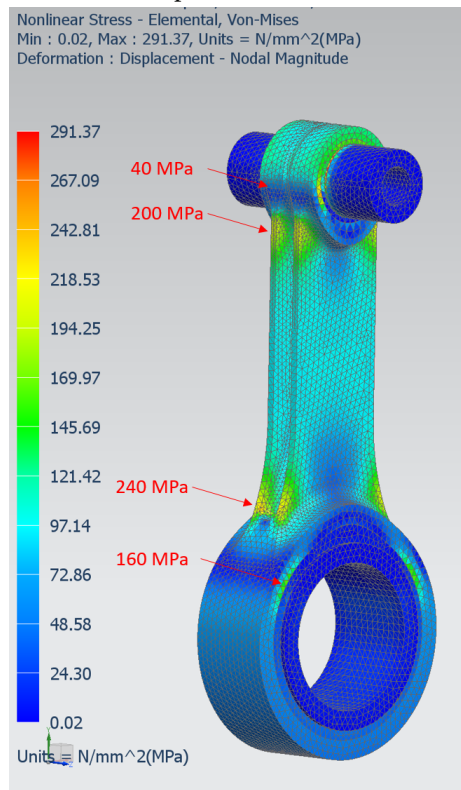


Figure 6.26: Von Mises stresses (KPI 5 and 6) - SOL 601.

6.3.3 Comparison

The comparison the results from the two solvers are done according to the KPI's defined in Chapter 3, as well as other highlighted parts (especially for tension stress).

LC1 comparison

Figure 6.27 shows the the ovalisation graphs of the big end in comparison to each other. As seen, they match relative good at both peaks. There are however evident that the bottom deformation (at 270 degrees) of the big end are greater according to the SOL 601 solver.

The small end ovalisation shows a greater relative deviation between the two solvers. Especially at the 270 degree deformation, where the SOL 101 shows less than half of the deformation compared to SOL 601.

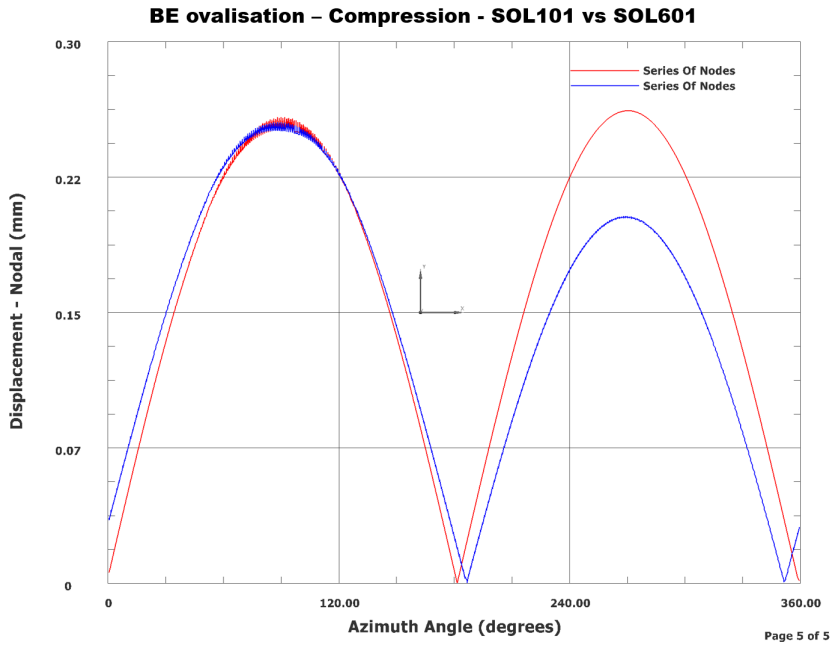


Figure 6.27: Displacement graph of the big end ovalisation under compression.

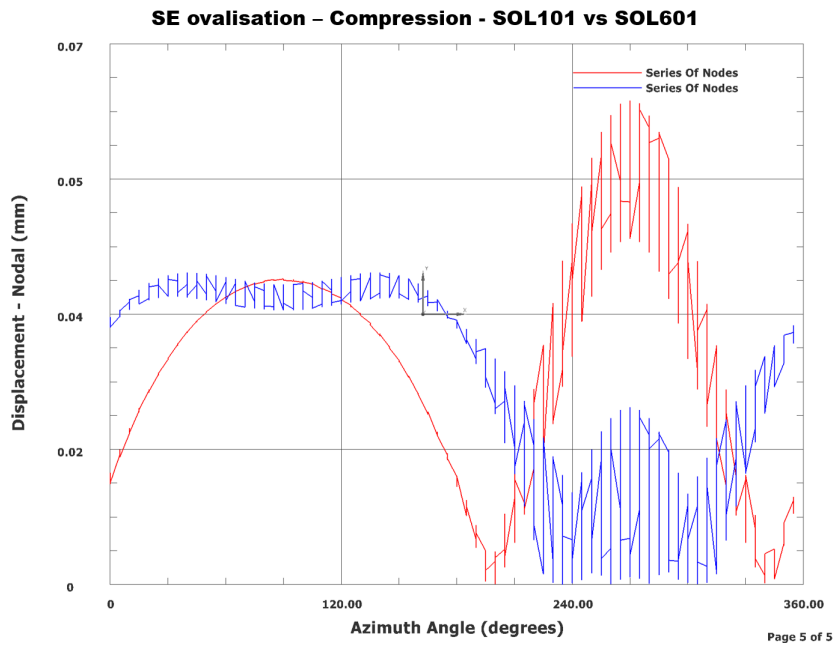


Figure 6.28: Displacement graph of the small end ovalisation under compression.

Table 6.1 shows a comparison of the KPI's from the two solvers. As seen, KPI 1 is fairly similar on both cases. The other KPI's shows a large deviation. This deviation can partly be explained in unrealistically high stress concentrations in the Small End edge. KPI 3 and 6, however, shows realistically states and gives a good reflection on the differences between the solvers.

KPI	SOL101 LC1	SOL601 LC1
1 - Max BE deformation	0.2554 mm	0.2618 mm
2 - Max SE deformation	0.0229 mm	0.0630 mm
3 - BE contact pressure	280 MPa	180 MPa
4 - SE contact pressure	500 MPa	300 MPa
5 - Max Von Mises	1833 MPa	866 MPa
6 - Max transition stress	650 MPa	570 MPa

Table 6.1: Comparison of KPI's from Load Case 1.

LC2 comparison

Similarly, the LC2 ovalisation graphs for both solvers are shown in Figure 6.29 and 6.30. It can be seen from Figure 6.29 that there exist an angle shift between the graphs. This is due to a small rotation that was observed in the SOL 101 results, consecutively leading to this shift. Further, it shows that the SOL 101 results give some higher values in the big end. The small end however, there exist a higher, as well as a more defined, peak in the SOL 601 results, where the SOL 101 results do not show any great indication of ovalisation.

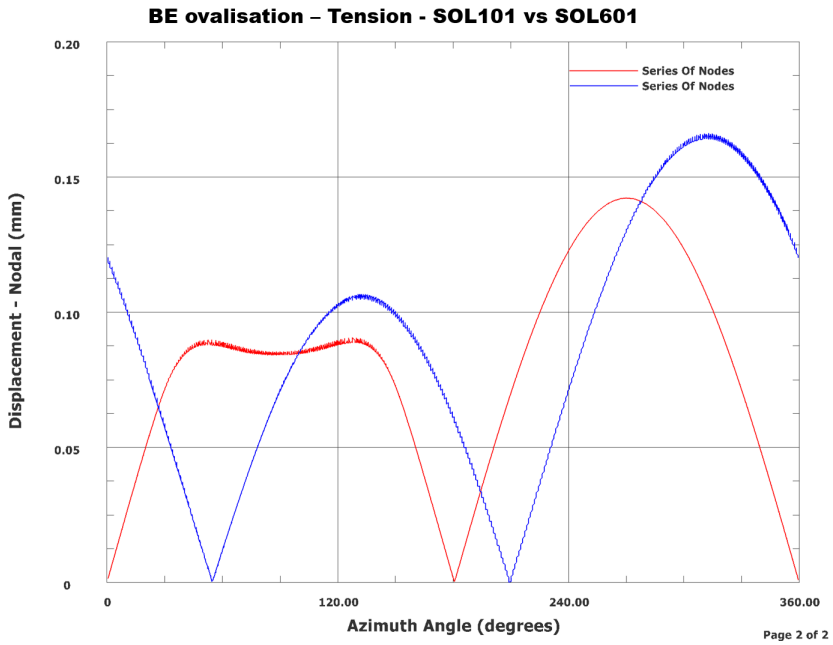


Figure 6.29: Comparison between the solvers, showing ovalisation of big end under tension

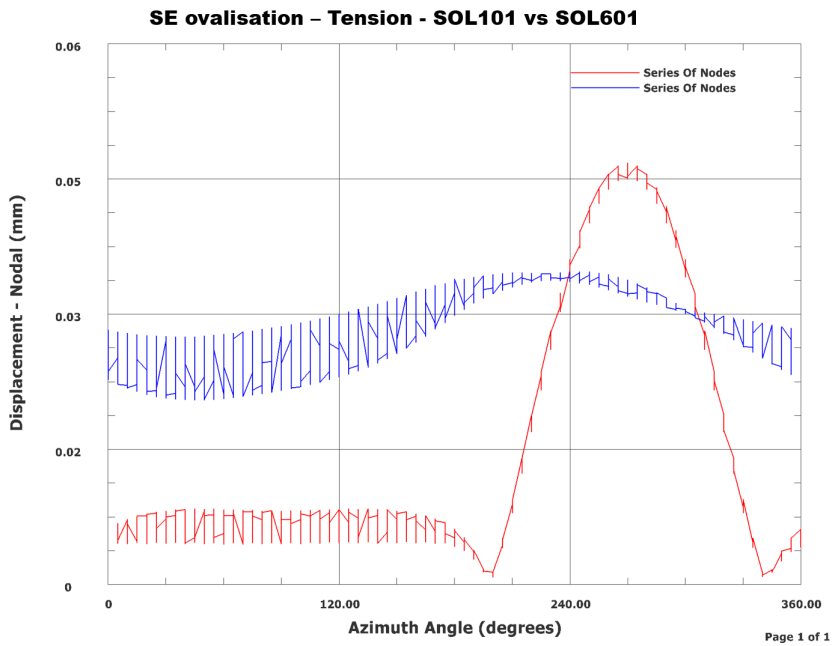


Figure 6.30: Comparison between the solvers, showing ovalisation of small end under tension

KPI	SOL101 LC2	SOL601 LC2
1 - Max BE deformation	0.1661 mm	0.1423 mm
2 - Max SE deformation	0.0326 mm	0.0468 mm
3 - BE contact pressure	30 MPa	30 MPa
4 - SE contact pressure	90 MPa	70 MPa
5 - Max Von Mises	430 MPa	291 MPa
6 - Max transition stress	300 MPa	40 MPa

Table 6.2: Comparison of KPI's from Load Case 2.

Table 6.2 reveals a fairly similar deformation of the two ends, as mentioned. Also, the contact pressures are of similar magnitude, with some deviations in the big end. Regarding KPI 5 and 6, however, it is clearly some differences between the results. As cited above, the SOL 601 results showed other stressed areas, than the SOL 101 solver. This is evident from Figure 6.26.

Chapter 7

Product Template Analysis

With regards to streamlining the designing and analysis process, a template has been made to easily initiate a contact analysis of the connecting rod. Both the SOL 101 and SOL 601 solvers was implemented in the template, such that the user has the option to choose the desired solver.

In order to create a analysis template in Product Template Studios, a sim-file has to be created first, which is then loaded into the PTS. This activates different pre/post features which is not available with just the part-file. Furthermore, a *Post View* has to be saved as a template in the *Post Processing Navigator*.

7.1 Post View Templates

A post view has to be defined as a template, in order to get a visual representation of the simulation performed in a Product Template Analysis. This can be a plot of the deformation, stresses etc., depending on the *Output Request* defined before the simulation.

For this propose, a plot of the deformation with respect to the two cylindrical nodal displacement coordinate systems, would give a good understanding of the ovalisation. Also, contact pressure would be beneficial for ovalisation analysis. Max Von Mises stresses are also included as a *Post View* template.

7.2 Product Template Design

When the sim-file is imported into the PTS, a simple drag-and-drop approach is used to add the desirable solutions, mesh-control and other controls, as seen in Figure 7.1. Thus, building the template systematically.

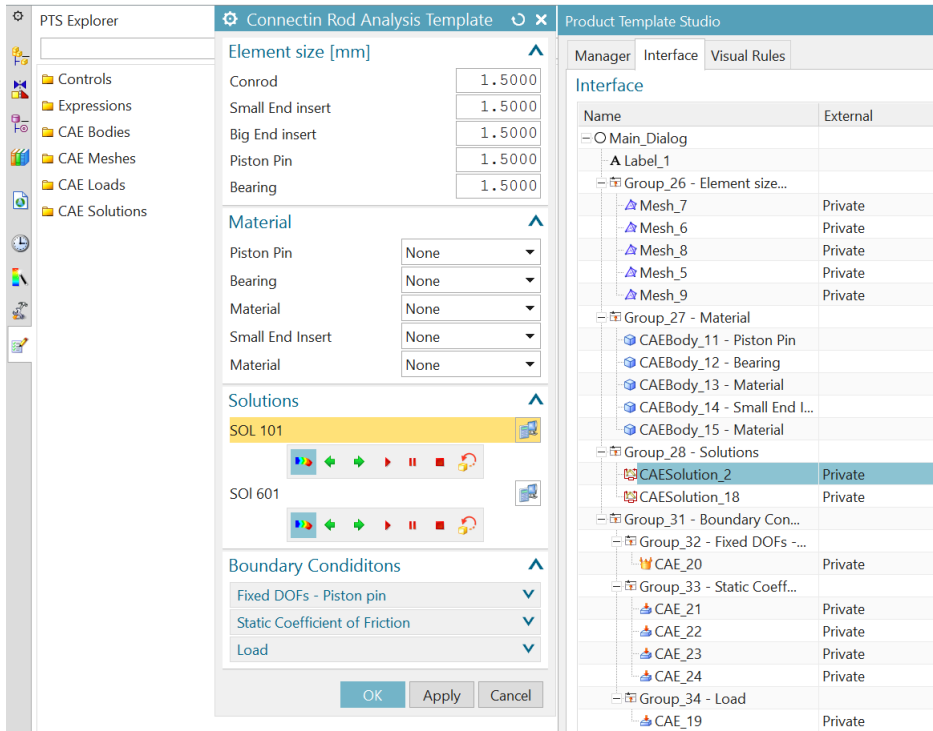


Figure 7.1: Designing the template.

The following were added to this template:

- **Expressions** - Controls the implementation of pre-defined expressions.
- **CEA Bodies** - Controls the material of the different solids in the model.
- **CEA Meshes** - Controls the mesh, e.g the element size.
- **CEA Loads** - Controls the applied loads, constraints and the *Simulation Objects*, e.g. the contact formulation.
- **CEA Solution** - Controls the available solution methods/solvers.

Within each of these controls, there are several options to enable various features. After a careful review of the different options, those who seemed most valuable for this kind of applications were chosen and implemented in the template.

Regarding the contact parameters, there were only possible to influence the static coefficient of friction, and not the other (nonlinear) parameters. Therefore, it were defined four *expressions* to be able to assign interference and play to the model. As mentioned earlier, these values are given to the specific regions. To be able to parametrically control these values, the defined expression is entered, as opposed to a number. Further, as the play-value has to be of a negative order, this may cause for some confusion in the template. An inverse expression was created to invert the play-value, thus resulting in a positive value in the FEA template.

7.3 The FEA Template

The template is accessed through the *Assembly Navigator* in the *Modelling* application. By right-clicking the symbol next to the part-name, the template opens up, together with the FE model. Figure 7.2 shows the resulting FEA template.

First option in the template, is the element size. Each part of the model can be assigned an individual element size by entering the desired value in the fields. By changing the value, and pressing *Apply*, NX generates a new mesh and updates the FE model accordingly.

Secondly, the material selection gives the user the option to assign materials to the model, which can be any material stored in the local library. Further, boundary conditions are defined. This includes the force (in y-direction), static coefficient of friction between the four contact surfaces, and the interference and play between the same surfaces.

At last, the user has the option to choose between which solver to use. In this template, the SOL 101 and 601 solver are added. However, it is possible to add any solver available in NX. By clicking the symbol next to the desired solver, NX starts the solution process as usual.

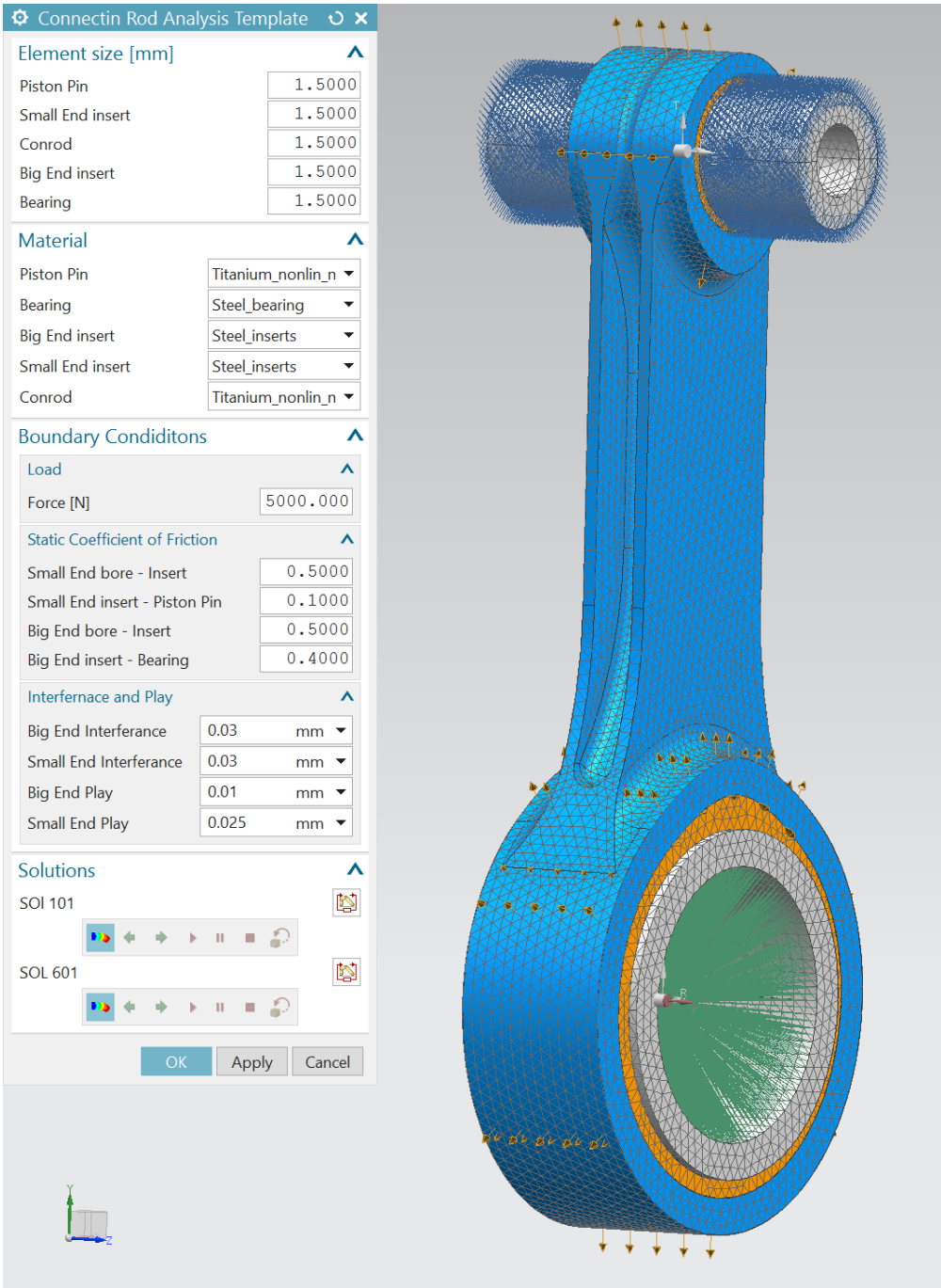


Figure 7.2: The FEA template.

For demonstrations purposes, an SOL 101 analysis is performed through the template, with a 3 mm element size. Figure 7.3 shows the result of the analysis. By clicking the animation symbol, the animated results are displayed. Depending on which *Post View* templates where created, the user can switch between the different views, displaying plots from displacement output, contact pressure and Von Mises stresses.

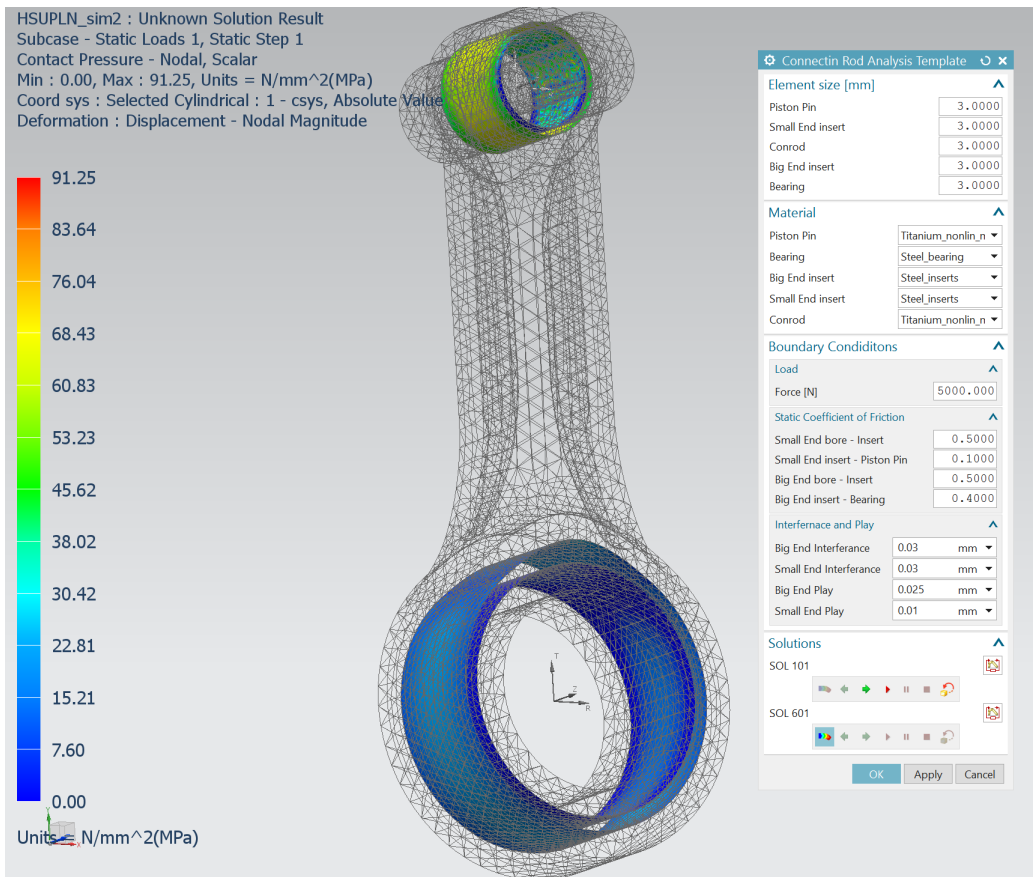


Figure 7.3: FEA results from the template.

Unfortunately, its not possible to show graphs from these results, as was done in the ovalisation analysis. Rendering it more difficult to quantify the ovalisation. Nonetheless, a displacement animation of the deformation with respect to the assigned cylindrical nodal coordinate systems. This results in a good representation of the ovalisation, as seen in Figure 7.4.

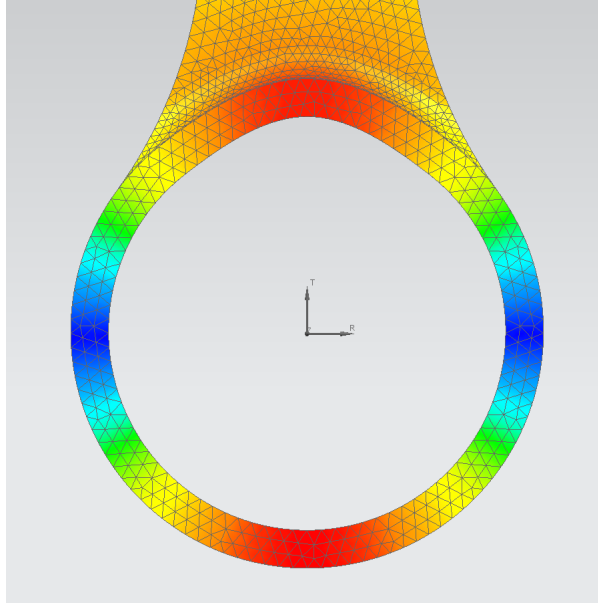


Figure 7.4: Displacement of big end bore with respect to the cylindrical coordinate system.

Shown in the figure above, it can easily be observed the ovalisation that occurs in the big end bore. Similar post view is created for the small end deformation.

7.3.1 Editing the model

If desired, the user can do design changes to the model, and afterwards open the template and run an analysis. Upon entering the FEA template, NX generates a new mesh adapting to the new geometry created, and displays the new FE model. Thus, the user can do design modification to the model, and verify the new design with a quick and easy simulation set-up.

Chapter 8

Challenges

Through this thesis work, there has occurred various challenges and obstacles. Some of which has been discussed through the text, such as the appearance of distorted elements due to automatic face mating.

As described in 1.3 Objectives and 1.5 Vision, it was desired to make a single template for several connecting rod designs, by combining a modelling template with a FEA template. As the PTS needs a single sim-file to be imported to build the template, consequently this demands that all the connecting rods are in the same sim-file. Further, each conrod has to be assigned its own individual FE model. A regular fem-file would not be able to differ from the various FE models, and generates a new mesh when a new body is selected. This was solved by generating an assembly of the various designs, and further a assembly-fem, keeping everything in a single fem-file, and thus a single sim-file. However, upon importing the sim-file to the PTS, it seemed not to be available for import. Searching for an explanation for this in the documentation, and online, was unsuccessful. It seems that the current PTS module does not support sim-files created by assemblies.

The nonlinear solver SOL 601 also prompted some difficulties. The contact conditions introduced in this problem, made the solver sensitive for non-convergence of the solution. Several attempts was made, with various contact formulations and solution parameters, until the solver successfully reached convergence in all time steps and where completed.

Chapter 9

Conclusion and Suggestions for Further Work

9.1 Conclusions

Generally, it can be seen from the results that there are various deviations between the SOL 101 and 601 solvers. Especially with regards to KPI 3 through 6 in Load Case 1, regarding contact pressure and Von Mises stress, as well as KPI 5 and 6 in Load Case 2. From Table 6.2 it is observed that the deformation in the two ends, are not so different, however it is evident from the graphs that the SOL 101 does not capture the ovalisation of the Small End so successfully. Also, as was observed in the stress results of Load Case 2, the two solver had some differences regarding stress concentrations.

With this in mind, it is indisputable that the SOL 601 solver offers a greater accuracy of the results and should be applied to contact problems. The advantage of specifying detailed nonlinear contact parameters, results in a more refined solution.

A mapping of the parameters crucial for contact convergence and general nonlinear stability was established. The following were found to be essential for a successful nonlinear contact analysis:

- Add friction
- Use small displacement instead of large
- Incrementally remove the initial penetrations
- Define Contact Compliance
- Use more iterations
- Smaller time steps
- Use Automatic Time Stepping

By tweaking these parameters, a stable SOL 601 simulation can be achieved.

It can, however, be seen from the comparison graphs that the big end deformation does not differ greatly between the different solvers. And with a drastically decreased simulation time, the SOL 101 solver would be preferable in such isolated applications.

Regarding the Product Template Analysis, the generated template offers a quick and intuitive way to do contact analysis of the connecting rod. Several animated post views can be implemented to give the user the desired feedback, but the PTS does not support other kinds of output than animations. It could be more valuable for the user to be able to retrieve more quantifiable information, such as the graphs presented in this thesis. Also, its currently only the static coefficient of friction parameter that is available for modification. The advanced nonlinear parameters are not accessible in the PTS. Thus, a complete control of the contact formulations is not possible through the template. This diminish some of the advantages of using the SOL 601 solver, compared with the SOL 101 solver, in the current version of PTS.

9.2 Suggestions for further work

During this project, several other aspects has proven to be of interest and are considered as a natural extension of the work presented in this report. These suggestions are listen below:

- A thorough comparison of the different suggested simplified bearing models.
- A more comprehensive analytically approach to establish the material properties of the substituting bearing model.
- Introduction of other load cases, e.g. with several force components.
- A dynamic simulation (and corresponding template) of the connecting rod.
- Perform design modification and optimization based on the results presented in this thesis.
- Implementation of more solvers in the FEA template.
- If/when the PTS module in NX supports the use of assembly simulations, a complete implementation of several connecting rod designs and a combination of a modelling template for rapid design changes and a FEA template for quick and easy analysis set-up.
- Give the user other feedback from the template simulations, such as graphs, if/when this is available in future PTS modules.

Appendix A

Abbreviations

PTS Product Template Studio

GUI Graphical User Interface

CPU Central Processing Unit

RPM Revolutions Per Minute

Conrod Connecting Rod

BE Big End

SE Small End

FE Finite Element

FEM Finite Element Method

FEA Finite Element Analysis

COF Coefficient Of Friction

KPI Key Performance Indicators

Appendix B

Risk Assessment



ID	20239	Status	Dato
Risikoområde	Risikovurdering: Helse, miljø og sikkerhet (HMS)	Opprettet	18.05.2017
Opprettet av	Are Nøst	Vurdering startet	
Ansvarlig	Are Nøst	Tiltak besluttet	
		Avsluttet	

Risikovurdering av gjennomføring av masteroppgaven**Gyldig i perioden:**

1/15/2017 - 7/11/2020

Sted:

NTNU

Mål / hensikt

Vurdere risikoen tilknyttet masteroppgaven

Bakgrunn

Utførelse av masteroppgave

Beskrivelse og avgrensninger

Arbeidet består kun av kontorarbeid

Forutsetninger, antakelser og forenklinger

Forutsetter ingen risiko tilknyttet arbeid med CAD/CAE verktøy

Vedlegg

[Ingen registreringer]

Referanser

[Ingen registreringer]

att. Teje Rølvåg

Bibliography

- [1] Faraz Junejo. Theories of machines, degrees of freedom. Presentation Transcript, 2015.
- [2] B Babu, T Florence, M Punithavalli, and BR Rohit. Design and experimental analysis of optimization technique used in connecting rod. 2015.
- [3] Siemens Product Lifecycle Management Software Inc. Element library reference.
- [4] P Goncharov, I Artamonov, T Khalitov, S Denisikhin, and D Sotnik. *Engineering Analysis With NX Advanced Simulation*. Lulu Publishing Service.
- [5] About nx software. https://docs.plm.automation.siemens.com/tdoc/nx/11/nx_help/uid:id627651.
- [6] About nx software. https://docs.plm.automation.siemens.com/tdoc/nx/11/nx_helpuid:xid1128419
- [7] Siemens Product Lifecycle Management Software Inc. *Advanced Nonlinear Theory and Modeling Guide*.
- [8] ADINA RD Inc. Adina theory and modeling guide.
- [9] Károly Molná, Lászlóand Váradi, Gábor Bóday, Péter Zwierczyk, and László Oroszváy. Simplified modeling for needle roller bearings to analyze engineering structures by fem.
- [10] Emil Claesson. Modelling of roller bearings in abaqus. Master's thesis, Chalmers University of Technology.
- [11] Erik Adolfsson. Simplified finite element bearing modeling. Master's thesis, Uppsala University.

- [12] Terje Rølvåg and Matteo Bella. Dynamic test bench for motocross engines. Technical report, NTNU and MX Research and Development DEpartment, MXRR.
- [13] Abhijit Londhe, Vivek Yadav, and Aparajita Sen. Finite element analysis of connecting rod and correlation with test. Technical report, Mahindra Mahindra Ltd.